

# PNAS

www.pnas.org

1

2 **Main Manuscript for**

3 Optimum growth temperature declines with body size within fish  
4 species

5

6 Max Lindmark<sup>a,1</sup>, Jan Ohlberger<sup>b</sup>, Anna Gårdmark<sup>c</sup>

7

8 <sup>a</sup> Swedish University of Agricultural Sciences, Department of Aquatic Resources, Institute of  
9 Coastal Research, Skolgatan 6, Öregrund 742 42, Sweden

10 <sup>b</sup> School of Aquatic and Fishery Sciences (SAFS), University of Washington, Box 355020, Seattle,  
11 WA 98195-5020, USA

12 <sup>c</sup> Swedish University of Agricultural Sciences, Department of Aquatic Resources, Skolgatan 6,  
13 SE-742 42 Öregrund, Sweden

14 \* Max Lindmark, Swedish University of Agricultural Sciences, Department of Aquatic Resources,  
15 Institute of Marine Research, Turistgatan 5, Lysekil 453 30, Sweden, Tel.: +46(0)104784137

16 Email: [max.lindmark@slu.se](mailto:max.lindmark@slu.se)

17 **Author Contributions:** ML conceived the study; ML, JO, AG designed research; ML performed  
18 research with input from JO and AG; ML, JO, AG wrote the paper and contributed to revisions of  
19 the manuscript.

20 **Preprint Servers:** bioRxiv: <https://www.biorxiv.org/content/10.1101/2021.01.21.427580v1>

21 **Competing Interest Statement:** No

22 **Classification:** BIOLOGICAL SCIENCES, Ecology

23 **Keywords:** body growth, metabolic rate, consumption rate, temperature-size rule, metabolic  
24 theory of ecology

25 **This PDF file includes:**

26 Main Text  
27 Figures 1 to 4

28 **Abstract**

29 According to the temperature-size rule, warming of aquatic ecosystems is generally predicted to  
30 increase individual growth rates but reduce asymptotic body sizes of ectotherms. However, we  
31 lack a comprehensive understanding of how growth and key processes affecting it, such as  
32 consumption and metabolism, depend on both temperature and body mass within species. This  
33 limits our ability to inform growth models, link experimental data to observed growth patterns, and  
34 advance mechanistic food web models. To examine the combined effects of body size and  
35 temperature on individual growth, as well as the link between maximum consumption, metabolism  
36 and body growth, we conducted a systematic review and compiled experimental data on fishes  
37 from 59 studies that combined body mass and temperature treatments. By fitting hierarchical  
38 models accounting for variation between species, we estimated how these three processes scale  
39 jointly with temperature and body mass within species. We found that whole-organism maximum  
40 consumption increases more slowly with body mass than metabolism, and is unimodal over the  
41 full temperature range, which leads to the prediction that optimum growth temperatures decline  
42 with body size. Using an independent dataset, we confirmed this negative relationship between  
43 optimum growth temperature and size within fish species. Small individuals may therefore exhibit  
44 increased growth with initial warming, whereas larger conspecifics could be the first to experience  
45 negative impacts of warming on growth. These findings help advance mechanistic models of  
46 individual growth and food web dynamics and improve our understanding of how climate warming  
47 affects growth and size structure of aquatic ectotherms.

48 **Significance Statement**

49 Predicting organism responses to a warming climate requires understanding how physiological  
50 processes such as feeding, metabolism, and growth depend on body size and temperature.  
51 Common growth models predict declining optimum growth temperatures with body size if  
52 energetic costs (metabolism) increase faster than gains (feeding) with body size. However, the  
53 generality of these features has not been evaluated at the within-species level. By collating data  
54 on fish through a systematic literature review, we find support for both declining net energy gain  
55 and declining optimum growth temperatures with body size. This implies large individuals within  
56 populations may be the first to suffer poor growth due to warming, with consequences for  
57 fisheries yield and food web structure in warmer climates.

58 **Introduction**

59 Individual body growth is a fundamental process powered by metabolism, and thus depends on  
60 body size and temperature (1). It affects individual fitness and life history traits, such as  
61 maturation size, population growth rates (2), and ultimately energy transfer across trophic levels  
62 (3, 4). Therefore, understanding how growth scales with body size and temperature is important  
63 for predicting the impacts of global warming on the structure and functioning of ecosystems.

64 Global warming is predicted to lead to declining body sizes of organisms (5, 6). The temperature  
65 size-rule ('TSR') states that warmer rearing temperatures lead to faster developmental times (and  
66 larger initial size-at-age or size-at-life-stage), but smaller adult body sizes in ectotherms (7, 8).  
67 This relationship is found in numerous experimental studies (7), is reflected in latitudinal gradients  
68 (9), and is stronger in aquatic than terrestrial organisms (9, 10). Support for the TSR exists in  
69 fishes, in particular in young fish, where reconstructed individual growth histories often reveal  
70 positive correlations between growth rates and temperature in natural systems (11–14). However,  
71 whether the positive effect of warming on growth is indeed limited to small individuals within a  
72 species, as predicted by the temperature size-rule, is less clear. Negative correlations between  
73 maximum size, asymptotic size or size-at-age of old fish and temperature have been found in  
74 commercially exploited fish species (13, 15, 16). However, other studies, including large scale  
75 experiments, controlled experiments and latitudinal studies or observational data on unexploited  
76 species, have failed to find negative relationships between maximum size, growth of old fish or  
77

79 mean size and temperature (14, 17–20) and differences between species may be related to life  
80 history traits and depend on local environmental conditions (20, 21).

81  
82 While the support for TSR is mixed, and the underlying mechanisms are not well understood (8,  
83 22, 23), theoretical growth models, such as Pütter growth models (24), including the von  
84 Bertalanffy growth model (VBGM) (25), commonly predict declines in asymptotic body mass with  
85 temperature and declines in optimum growth temperature with body mass, in line with the TSR  
86 (26–28). Yet, the physiological basis of these models has been questioned, as the commonly  
87 applied scaling parameters (mass exponents) tend to differ from empirical estimates (29, 30).  
88 Hence, despite attempting to describe growth from first principles, Pütter growth models can also  
89 be viewed as phenomenological. In more mechanistic growth models, the difference between  
90 energy gain and expenditure is partitioned between somatic growth and gonads (31–34). Energy  
91 gain is normally the amount of energy extracted from consumed food and expenditure is defined  
92 as maintenance, activity and feeding metabolism. These components of the energetics of growth  
93 are found in dynamic energy budget models (32, 35), including physiologically structured  
94 population models (PSPMs) (36), and size-spectrum models (37–39). Therefore, it is important to  
95 understand how consumption and metabolism rates scale with body mass and temperature in  
96 order to understand if and how growth of large fish within populations is limited by temperature,  
97 and to evaluate the physiological basis of growth models.  
98

99 Moreover, the effect of body mass and temperature on growth dynamics should be evaluated  
100 over ontogeny at the intraspecific level (within species), which better represents the underlying  
101 process than interspecific data (among species) (30). For instance, we do not expect an  
102 interspecific relationship between optimum growth temperature and body mass, but within  
103 species it may have a large effect on growth dynamics. Despite this, intraspecific body mass and  
104 temperature scaling is often inferred from interspecific data, and we know surprisingly little about  
105 average relationship between consumption and metabolic exponents within species (30).  
106 Importantly, how physiological rates depend on mass and temperature within species can differ  
107 from the same relationships across species (40–42). Across species, rates are often assumed  
108 and found to scale as power functions of mass with exponents of 3/4 for whole organism rates (-  
109 1/4 for mass-specific rates), exponentially with temperature, and with independent mass and  
110 temperature effects (e.g., in the Arrhenius fractal supply model (AFS) applied in the metabolic  
111 theory of ecology, MTE (1, 43, 44)). In contrast, within species deviations from a general 3/4  
112 mass exponent are common (42, 45, 46), rates are typically unimodal (41, 47–49) and the effects  
113 of mass and temperature can be interactive (40, 50–53) (but see Jerde *et al.* (42)). Alternative  
114 approaches that overcome these obstacles include fitting multiple regression models where  
115 coefficients for mass and temperature are estimated jointly (44), as well as fitting non-linear or  
116 polynomial models that can capture the de-activation of biological rates at higher temperatures  
117 (47, 48, 54). This requires intraspecific data with variation in both mass and temperature.  
118

119 In this study, we analyze how maximum consumption, metabolism and growth rate of fish scale  
120 intraspecifically with mass and temperature. We performed a systematic literature review by  
121 searching the Web of Science Core Collection to compile datasets on individual-level maximum  
122 consumption, metabolism and growth rates of fish from experiments in which the effect of fish  
123 body mass is replicated across multiple temperatures within species (total n=3672, with data from  
124 13, 20 and 34 species for each rate, respectively). We then fit hierarchical Bayesian models to  
125 estimate general intraspecific scaling parameters while accounting for variation between species.  
126 The estimated mass dependence and temperature sensitivity of mass-specific consumption and  
127 metabolism are used to quantify average changes in net energy gain (and hence, growth,  
128 assumed proportional to net energy gain) over temperature and body mass. Lastly, we compare  
129 our predicted changes in optimum growth temperature over body mass with an independent

130 experimental dataset on optimum growth temperatures across individuals of different sizes within  
131 species.

132

### 133 Results

134 We identified that within species of fish, mass-specific metabolic rates increase faster with body  
135 mass than maximum consumption rates, and neither of these rates conform to the commonly  
136 predicted -1/4 scaling with body mass (Fig. 1). We also quantified the unimodal relationship of  
137 consumption rate over the full temperature range (Fig. 2). Combined, these scaling relationships  
138 lead to the prediction, based on Pütter-type growth models, that optimum growth temperature  
139 declines with body size (Fig. 3) (26). The prediction of declining optimum growth temperatures with  
140 size was confirmed by our analysis of independent experimental growth rate data. We find that  
141 within species the optimum growth temperature declines with body size by 0.31°C per unit increase  
142 in the natural log of relative body mass (Fig. 4). Below we present the underlying results in more  
143 detail.

144

145 We found that the average intraspecific mass exponent for mass-specific consumption rate is  
146 smaller (-0.38 [-0.46, -0.30]) than that for metabolic rate (-0.21 [-0.26, -0.16]), based on the non-  
147 overlapping Bayesian 95% credible intervals (Fig. 1). It is also probable that the mass-specific  
148 scaling exponents differ from -1/4 (that is predicted by the MTE), because > 99% of the posterior  
149 distribution of the mass exponent of maximum consumption is below -1/4, and 95% of the posterior  
150 distribution of the mass exponent of metabolic rate is above -1/4. Activation energies of maximum  
151 consumption rate and metabolism are both similar (0.69 [0.54, 0.85] and 0.62 [0.57, 0.67]  
152 respectively; Fig. 1) and largely fall within the prediction from the MTE (0.6-0.7 eV) (1)). The global  
153 intraspecific intercept for routine and resting metabolic rate is estimated to be -1.93 [-2.11, -1.74],  
154 and for standard metabolic rate it is -2.49 [-2.81, -2.17] (SI Appendix, Fig. S7). Models where all  
155 coefficients varied by species were favored in terms of WAIC (M5 and M1, for consumption and  
156 metabolism, respectively) (SI Appendix, Table S4). We found statistical support for a species-  
157 varying mass and temperature interaction for metabolic rate. 98% of the posterior distribution of  
158 the global interaction coefficient  $\mu_{\beta_3}$  is above 0 (SI Appendix, Fig. S5). The estimated coefficient is  
159 0.018 [0.0008, 0.0367] on the Arrhenius temperature scale, which corresponds to a decline in the  
160 mass scaling exponent of metabolic rate by 0.0026 °C<sup>-1</sup>. The selected model for maximum  
161 consumption rate did not include an interaction term (M5).

162

163 We estimated the parameters of the Sharpe-Schoofield equation (Eq. 4) for temperature-  
164 dependence of consumption including data beyond peak temperature as: activation energy,  $E_j =$   
165 0.58 [0.45, 0.74], rate at reference temperature,  $C_{0j} = 0.70 [0.52, 0.89]$ , temperature at which the  
166 rate is reduced to half (of the rate in the absence of deactivation) due to high temperatures,  $T_h =$   
167 4.03 [2.82, 4.98], and the rate of the decline past the peak,  $E_h = 2.64 [2.17, 3.22]$ . This shows that  
168 the relationship between consumption rate and temperature is unimodal and asymmetric, where  
169 the decline in consumption rate at high temperatures is steeper than the increase at low  
170 temperatures (Fig. 2).

171

172 The above results provide empirical support for the two criteria outlined in Morita et al., (26) that  
173 result in declining optimum temperatures with size, i.e. (i) smaller whole organism mass exponent  
174 for consumption than metabolism (Fig. 1) and (ii) that growth reaches an optimum over  
175 temperature. In our case, the second criterion is met because consumption reaches a peak over  
176 temperature (Fig. 2). We illustrate the consequence of these findings in Fig. 3, which shows that  
177 the optimum temperature for net energy gain is reached at a lower temperature for a smaller fish  
178 because of the difference in exponents and because net gain is unimodally related to temperature.

179 Assuming growth is proportional to net energy gain, this predicts that optimum growth temperature  
180 declines with body size.

181  
182 Using independent data from growth trials across a range of body sizes and temperatures, we also  
183 find strong statistical support for a decline in optimum growth temperature with body mass within  
184 species, because 92% of the posterior density of the global slope estimate ( $\mu_{\beta_1}$ ) is below 0. The  
185 models with and without species-varying slopes were indistinguishable in terms of WAIC (*SI*  
186 Appendix, Table S5), and we present the results for the species-varying intercept and slope model,  
187 due to slightly better model diagnostics (*SI Appendix*, Fig. S24-27). The global relationship is given  
188 by the model:  $T_{opt} = -0.074 - 0.31 \times m$ , where  $m$  is the natural log of the rescaled body mass,  
189 calculated as the species-specific ratio of mass to maturation mass.

190  
191 **Discussion**

192 In this study, we systematically analyzed the intraspecific scaling of consumption, metabolism  
193 and growth with body mass and temperature. We found strong evidence for declining optimum  
194 growth temperatures as individuals grow in size based on two independent approaches. First, we  
195 find differences in the intraspecific mass-scaling of consumption and metabolism, and a unimodal  
196 temperature dependence of consumption, which lead to predicted declines in optimum  
197 temperature for net energy gain (and hence growth) with size. Second, we confirm this prediction  
198 using intraspecific growth rate data of fish. Our analysis thus demonstrates the importance of  
199 understanding intraspecific scaling relationships when predicting responses of fish populations to  
200 climate warming.

201  
202 That warming increases growth and development rates but reduces maximum or adult size is well  
203 known from experimental studies, also referred to as the temperature-size rule (TSR). Yet, the  
204 mechanisms underlying the TSR remain poorly understood. Pütter-type growth models, including  
205 the von Bertalanffy growth equation (VBGE), predict that the asymptotic size declines with  
206 warming if the ratio of the coefficients for energy gains and losses ( $H/K$  in Eq. 7) (27) declines  
207 with temperature. However, the assumptions underlying the VBGE were recently questioned  
208 because of the lack of empirical basis for the scaling exponents and the effects of those on the  
209 predicted effects of temperature on asymptotic size (29, 30). Specifically, the allometric exponent  
210 of energy gains ( $a$ ) is assumed to be smaller than that of energetic costs ( $b$ ) (Eq. 7). This is  
211 based on the assumption that anabolism scales with the same power as surfaces to volumes  
212 ( $a = 2/3$ ) and catabolism, or maintenance metabolism, is proportional to body mass ( $b = 1$ ) (25,  
213 55). In contrast, maintenance costs are commonly thought to instead be proportional to standard  
214 metabolic rate, which in turn often is proportional to intake rates at the interspecific level (1, 30).  
215 This leads to  $a \approx b$ , resulting in unrealistic growth trajectories and temperature dependences of  
216 growth dynamics in Pütter models (29, 30). However, similar to how the existence of large fishes  
217 in tropical waters does not invalidate the hypothesis that old individuals of large-bodied fish may  
218 reach smaller sizes with warming, interspecific scaling parameters cannot reject or support these  
219 model predictions on growth within species. We show that the average intraspecific whole-  
220 organism mass scaling exponent of metabolism is larger than that of maximum consumption, i.e.,  
221 the inequality  $a < b$  holds at the intraspecific level. This implies that on average within species of  
222 fish, energetic costs increase faster with body mass than gains (all else equal). Importantly, when  
223 accounting for this difference in the exponents, and the unimodal thermal response of  
224 consumption, the thermal response of net energy gain is characterized by the optimum  
225 temperature being a function of body size (26). Therefore, empirically derived intraspecific  
226 parameterizations of simple growth models result in predictions in line with the TSR, in this case  
227 via declines in optimum growth temperatures over ontogeny rather than declines in asymptotic  
228 sizes.

229  
230 Declines in optimum growth temperatures over ontogeny as a mechanism for TSR-like growth  
231 dynamics do not rely on the assumption that the ratio of the coefficients for energy gains and  
232 losses declines with temperature. In fact, we find that when using data from sub-peak

temperatures only, the average intraspecific predictions about the activation energy of metabolism and consumption do not differ substantially, which implies there is no clear loss or gain of energetic efficiency with warming within species. This is in contrast to other studies, e.g. Lemoine & Burkepile (56) and Rall *et al.* (57). However, it is in line with the finding that growth rates increase with temperature (e.g. 58), which is difficult to reconcile from a bioenergetics perspective if warming always reduced net energy gain. Our analysis instead suggests that the mismatch between gains and losses occurs when accounting for unimodal consumption rates over temperature. The match, or mismatch, between the temperature dependence of feeding vs. metabolic rates is a central question in ecology that extends from experiments to meta-analyses to food web models (56, 57, 59–61). Our study highlights the importance of accounting for non-linear thermal responses for two main reasons. First, the thermal response of net energy gain reaches a peak at temperatures below the peak for consumption. Secondly, as initial warming commonly leads to increased growth rates, the effect of warming on growth rates should depend on temperature rather than growth being assumed to be monotonically related to temperature.

Life-stage dependent optimum growth temperatures have previously been suggested as a component of the TSR (8). Although previous studies have found declines in optimum growth temperatures with body size in some species of fishes and other aquatic ectotherms (62–66), others have not (67, 68). Using systematically collated growth data from experiments with variation in both size and temperature treatments (13 species), we find that for an average fish, the optimum growth temperature declines as it grows in size. This finding emerges despite the small range of body sizes used in the experiments (only 10% of observations are larger than 50% of maturation size) (*SI Appendix*, Fig. S2). Individuals of such small relative size likely invest little energy in reproduction, which suggests that physiological constraints contribute to reduced growth performance of large compared to small fish, in addition to increasing investment into reproduction (69).

Translating results from experimental data to natural systems is challenging because maximal feeding rates, unlimited food supply, lack of predation, and constant temperatures do not reflect natural conditions, yet affect growth rates (67, 70, 71). In addition, total metabolic costs in the wild also include additional costs for foraging and predator avoidance. It is, however, typically found and assumed that standard metabolic rate and natural feeding levels are proportional to routine metabolic rate and maximum consumption rate, respectively, and thus exhibit the same mass-scaling relationships (32, 72). Intraspecific growth rates may not appear to be unimodally related to temperature when measured over a temperature gradient across populations within a species (20), because each population can be adapted to local climate conditions and thus display different temperature optima. However, each population likely has a thermal optimum for growth, which differs between individuals of different size. Hence, each population might have a unimodal relationship with temperature as it warms. This highlights the importance of understanding the time scale of environmental change in relation to that of immediate physiological responses, acclimation, adaptation and community reorganization for the specific prediction about climate change impacts.

In natural systems, climate warming may also result in stronger food limitation (71, 73). Hence, as optimum growth temperatures decline not only with size but also food availability (67, 74), and realized consumption rates are a fraction of the maximum consumption rate (20–70%) (Kitchell *et al.* 1977; Neuenfeldt *et al.* 2019), species may be negatively impacted by warming even when controlled experiments show they can maintain growth capacity at these temperatures. Supporting this point is the observation that warming already has negative or lack of positive effects on body growth in populations living at the edge of their physiological tolerance in terms of growth (12, 14).

Whether the largest fish of a population will be the first to experience negative effects of warming, as suggested by our finding that optimum growth temperature declines with body size, depends

287 on the environmental temperatures they typically experience compared to smaller conspecifics.  
288 They may for instance inhabit colder temperatures compared to small fish due to ontogenetic  
289 habitat shifts (75, 76); see also Heincke's law (77, 78). That said, there is already empirical  
290 evidence of the largest individuals in natural populations being the first to suffer from negative  
291 impacts of warming from heatwaves (79), or not being able to benefit from warming (14, 18).  
292 Hence, assuming that warming affects all individuals of a population equally is a simplification  
293 that can bias predictions of the biological impacts of climate change.

294  
295 The interspecific scaling of fundamental ecological processes with body mass and temperature  
296 has been used to predict the effects of warming on body size, size structure, and population and  
297 community dynamics (26, 59, 80, 81). We argue that a contributing factor to the discrepancy  
298 between mechanistic growth models, general scaling theory, and empirical data has been the  
299 lack of data synthesis at the intraspecific level. The approach presented here can help overcome  
300 limitations of small data sets by borrowing information across species in a single modelling  
301 framework, while accounting for the intraspecific scaling of rates. Accounting for the faster  
302 increase in whole-organism metabolism than consumption with body size, the unimodal thermal  
303 response of consumption, and resulting size-dependence of optimum growth temperatures is  
304 essential for understanding what causes observed growth responses to global warming.  
305 Acknowledging these mechanisms is also important for improving predictions on the  
306 consequences of warming effects on fish growth for food web functioning, fisheries yields and  
307 global food production in warmer climates.

308

## 309 Materials and Methods

### 310 Data acquisition

311 We searched the literature for experimental studies evaluating the temperature response of  
312 individual maximum consumption rate (feeding rate at unlimited food supply, *ad libitum*), resting,  
313 routine and standard oxygen consumption rate as a proxy for metabolic rate (82) and growth  
314 rates across individuals of different sizes within species. We used three different searches on the  
315 Web of Science Core Collection (see *SI Appendix*, for details). In order to estimate how these  
316 rates depend on body size and temperature within species, we selected studies that  
317 experimentally varied both body size and temperature (at least two temperature treatments and at  
318 least two body masses). The average number of unique temperature treatments (temperature  
319 rounded to nearest °C) by species is 7.2 for growth and 4.3 for consumption and metabolism  
320 data). The criteria for both mass and temperature variation in the experiments reduces the  
321 number of potential data sets, as most experimental studies use either size or temperature  
322 treatments, not both. However, this criterion allows us to fit multiple regression models and  
323 estimate the effects of mass and temperature jointly, and to evaluate the probability of interactive  
324 mass- and temperature effects within species. Following common practice we excluded larval  
325 studies, which represents a life stage exhibiting different constraints and scaling relationships  
326 (40).

327  
328 Studies were included if (i) a unique experimental temperature was recorded for each trial ( $\pm 1^\circ\text{C}$ ),  
329 (ii) fish were provided food at *ad libitum* (consumption and growth data) or if they were unfed  
330 (resting, standard or routine metabolic rate), and (iii) fish exhibited normal behavior during the  
331 experiments. We used only one study per species and rate to ensure that all data within a given  
332 species are comparable as measurements of these rates can vary between studies due to e.g.  
333 measurement bias, differences in experimental protocols, or because different populations were  
334 studied (42, 83). In cases where we found more than one study for a given rate and species, we  
335 selected the most suitable study based on our pre-defined criteria (for details, see *SI Appendix*).  
336 We ensured that the experiments were conducted at ecologically relevant temperatures (*SI*  
337 *Appendix*, Figs. S1, S3). A more detailed description of the search protocol, data selection,  
338 acquisition, quality control, collation of additional information and standardizing of rates to  
339 common units can be found in *SI Appendix*.

341 We compiled four datasets: maximum consumption rate, metabolic rate, growth rate and the  
 342 optimum growth temperature for each combination of body mass group and species. We  
 343 compiled a total of 746 measurements of maximum consumption rate (of which 666 are below  
 344 peak), 2699 measurements of metabolic rate and 227 measurements of growth rate (45 optimum  
 345 temperatures) from published articles for each rate, from 20, 34 and 13 species, respectively,  
 346 from different taxonomic groups, habitats and lifestyles (Table S1-S2). We requested original data  
 347 from all corresponding authors of each article. In cases where we did not hear from the  
 348 corresponding author, we extracted data from tables or figures using Web Plot Digitizer (84).  
 349

### 350 Model fitting

#### 351 Model description

352 To each dataset, we fit hierarchical models with different combinations of species-varying  
 353 coefficients, meaning they are estimated with shrinkage. This reduces the influence of outliers  
 354 which could occur in species with small samples sizes (85, 86). The general form of the model is:

$$y_{ij} \sim N(\mu_{ij}, \sigma) \quad (1)$$

$$\mu_{ij} = \beta_{0j} + \sum_{p=1}^n (\beta_p \times x_{ip}) \quad (2)$$

$$\beta_{0j} \sim N(\mu_{\beta_0}, \sigma_{\beta_0}) \quad (3)$$

355 where  $y_{ij}$  is the  $i$ th observation for species  $j$  for rate  $y$ ,  $\beta_{0j}$  is a species-varying intercept,  $x_{ip}$  is a  
 356 predictor and  $\beta_p$  is its coefficient, with  $p = 1, \dots, n$ , where  $n$  is the number of predictors considered  
 357 in the model (mass, temperature, and their interaction). Predictors are mean centered to improve  
 358 interpretability (87). Species-level intercepts follow a normal distribution with hyperparameters  
 359  $\mu_{\beta_0}$  (global intercept) and  $\sigma_{\beta_0}$  (between-species standard deviation). For most models we also  
 360 allow the coefficient  $\beta_p$  to vary between species, such that  $\beta_p$  becomes  $\beta_{pj}$  and  $x_{ip} x_{ijp}$ , where  
 361  $\beta_{pj} \sim N(\mu_{\beta_p}, \sigma_{\beta_p})$ . For each dataset, we evaluate multiple combinations of species-varying  
 362 coefficients (from varying intercept to  $n$  varying coefficients). We used a mix of flat, weakly  
 363 informative, and non-informative priors. For the temperature and mass coefficients we used the  
 364 predictions from the MTE as the means of the normal prior distributions (1), but with large  
 365 standard deviations (see SI Appendix, Table S3). Below we describe how the model in Eqns. 1-3  
 366 is applied to each data set.

367

#### 368 Mass- and temperature dependence of consumption, metabolism and growth below peak 369 temperatures

370 Peak temperatures (optimum in the case of growth) refer to the temperature at which the rate was  
 371 maximized, by size group. For data below peak temperatures, we assumed that mass-specific  
 372 maximum consumption rate, metabolism and growth scale allometrically (as a power function of  
 373 the form  $I = i_0 M^{b_0}$ ) with mass, and exponentially with temperature. Hence, after log-log (natural  
 374 log) transformation of mass and the rate, and temperature in Arrhenius temperature ( $1/kT$  in unit  
 375  $eV^{-1}$ , where  $k$  is Boltzmann's constant [ $8.62 \times 10^{-5} eV K^{-1}$ ]), the relationship between the rate and  
 376 its predictors becomes linear. This is similar to the MTE, except that we estimate all coefficients  
 377 instead of correcting rates, and allow not only the intercepts but also slopes to vary across  
 378 species.

379

380 When applied to Eqns. 1-3,  $y_{ij}$  is the  $i$ th observation for species  $j$  of the natural log of the rate  
 381 (consumption, metabolism or growth), and the predictors are  $m_{ij}$  (natural log of body mass),  $t_{A,ij}$   
 382 (Arrhenius temperature,  $1/kT$  in unit  $eV^{-1}$ ), both of which were mean-centered, and their  
 383 interaction. Body mass is in g, consumption rate in  $g g^{-1} day^{-1}$ , metabolic rate in  $mg O_2 g^{-1} h^{-1}$   
 384 and specific growth rate in unit  $\% day^{-1}$ . We use resting or routine metabolism (mean oxygen  
 385 uptake of a resting unfed fish only showing some spontaneous activity) and standard metabolism  
 386 (resting unfed and no activity, usually inferred from extrapolation or from low quantiles of routine  
 387 metabolism, e.g. lowest 10% of measurements) to represent metabolic rate (88, 89). Routine and  
 388 resting metabolism constitute 58% of the data used and standard metabolism constitutes 42%.  
 389 We accounted for potential differences between these types of metabolic rate measurements by  
 390 adding two dummy coded variables,  $type_r$  and  $type_s$ , the former taking the value 0 for standard  
 391 metabolism and 1 for resting metabolism, and the latter taking the value 0 for standard  
 392 metabolism and 1 for standard metabolism. We included these variables in the model to account  
 393 for the difference in metabolism between resting and standard metabolism, and to account for the  
 394 difference in metabolism between routine and standard metabolism.

394 and 1 for a routine or resting metabolic rate measurement, and vice versa for the latter variable.  
 395 Thus, for metabolism, we replace the overall intercept  $\beta_{0j}$  in Eqns. 2-3 with  $\beta_{0rj}$  and  $\beta_{0sj}$ .  $\beta_{0sj}$  is  
 396 forced to 0 for a species that has a routine or resting metabolic rate and vice versa. We assume  
 397 these coefficients vary by species following normal distributions with global means  $\mu_{\beta_{0r}}$  and  $\mu_{\beta_{0s}}$ ,  
 398 and standard deviations  $\sigma_{\beta_{0r}}$  and  $\sigma_{\beta_{0s}}$ , i.e.  $\beta_{0rj} \sim N(\mu_{\beta_{0r}}, \sigma_{\beta_{0r}})$  and  $\beta_{0sj} \sim N(\mu_{\beta_{0s}}, \sigma_{\beta_{0s}})$ .  
 399

400 *Mass- and temperature dependence of consumption including beyond peak temperatures*  
 401 Over a large temperature range, many biological rates are unimodal. We identified such  
 402 tendencies in 10 out of 20 species in the consumption data set. To characterize the decline in  
 403 consumption rate beyond peak temperature, we fit a mixed-effects version of the Sharpe  
 404 Schoolfield equation (54) as parameterized in (90), to equations 1-2 with  $y_{ij}$  as rescaled  
 405 consumption rates ( $C$ ). Specifically, we model  $\mu_{ij}$  in Eq. 1 with the Sharpe-Schoolfield equation:

$$\mu_{ij} = \frac{C_{0j}(T_c)e^{E_j\left(\frac{1}{kT_c} - \frac{1}{kT}\right)}}{1 + e^{E_h\left(\frac{1}{kT_h} - \frac{1}{kT}\right)}} \quad (4)$$

$$E_j \sim N(\mu_E, \sigma_E) \quad (5)$$

$$C_{0j} \sim N(\mu_{C_0}, \sigma_{C_0}) \quad (6)$$

406 where  $C_{0j}(T_c)$  is the rate at a reference temperature  $T_c$  in Kelvin [K] (here set to 263.15),  $E_j$  [eV] is  
 407 the activation energy,  $E_h$  [eV] characterizes the decline in the rate past the peak temperature and  
 408  $T_h$  [K] is the temperature at which the rate is reduced to half (of the rate in the absence of  
 409 deactivation) due to high temperatures. We assume  $E_j$  and  $C_{0j}$  vary across species according to  
 410 a normal distribution with means  $\mu_E$  and  $\mu_{C_0}$ , and standard deviations  $\sigma_E$  and  $\sigma_{C_0}$  (Eq. 5-6). Prior  
 411 to rescaling maximum consumption (in unit g day<sup>-1</sup>) by dividing  $C_{ij}$  with the mean within species  
 412  $\bar{C}_j$ , we mass-normalize it by dividing it with  $m^a$  where  $m$  is mass in g and  $a$  is the whole-organism  
 413 mass-exponent calculated from the estimated mass-specific exponent with the log-linear model  
 414 fitted to data below peak temperature. Temperature,  $T$ , is centered by subtracting the  
 415 temperature at peak consumption estimated separately for each species using a linear model  
 416 with a quadratic temperature term. The rescaling is done to control for differences between  
 417 species with respect to the experimental temperatures relative to the temperature that maximizes  
 418 their consumption rate such that data can be pooled.

419 *Mass-dependence of optimum growth temperature*  
 420 To evaluate how the optimum temperature ( $t_{opt,ij}$ , in degrees Celsius) for individual growth  
 421 depends on body mass, we fit Eqns. 1-3 with  $y_{ij}$  as the mean-centered optimum growth  
 422 temperature within species ( $t_{opt,ij} = T_{opt,ij} - \bar{T}_{opt,j}$ ), to account for species being adapted to  
 423 different thermal regimes.  $m_{ij}$ , the predictor variable for this model, is the natural log of the ratio  
 424 between mass and mass at maturation within species:  $m_{ij} = \ln(M_{ij}/M_{mat,j}) - \bar{\ln}(M_{ij}/M_{mat,j})$ .  
 425 This rescaling is done because we are interested in examining relationships within species over  
 426 “ontogenetic size”, and because we do not expect an interspecific relationship between optimum  
 427 growth temperature and body mass because species are adapted to different thermal regimes.  
 428 We consider both the intercept and the effect of mass to potentially vary between species.

429 *Parameter estimation*  
 430 We fit the models in a Bayesian framework, using R version 4.0.2 (91) and JAGS (92) through the  
 431 R-package ‘rjags’ (93). We used 3 Markov chains with 5000 iterations for adaptation, followed by  
 432 15000 iterations burn-in and 15000 iterations sampling where every 5<sup>th</sup> iteration saved. Model  
 433 convergence was assessed by visually inspecting trace plots and potential scale reduction factors  
 434 ( $\hat{R}$ ) (SI Appendix).  $\hat{R}$  compares chain variance with the pooled variance, and values <1.1 suggest  
 435 all three chains converged to a common distribution (94). We relied heavily on the R packages  
 436 within ‘tidyverse’ (95) for data processing, as well as ‘ggmcmc’ (96), ‘mcmcvis’ (97) and  
 437 ‘bayesplot’ (98) for visualization.

443  
 444 *Model comparison*  
 445 We compared the parsimony of models with different hierarchical structures, and with or without  
 446 mass-temperature interactions, using the Watanabe-Akaike information criterion (WAIC) (99,  
 447 100), which is based on the posterior predictive distribution. We report WAIC for each model  
 448 described above (Table S4-S5), and examine models with  $\Delta$ WAIC values < 2, where  $\Delta$ WAIC is  
 449 each models difference to the lowest WAIC across models, in line with other studies (101).  
 450  
 451 *Net energy gain*  
 452 The effect of temperature and mass dependence of maximum consumption and metabolism  
 453 (proportional to biomass gain and losses, respectively) (31, 32, 34) on growth is illustrated by  
 454 visualizing the net energy gain. The model for the net energy gain (growth) can be viewed as a  
 455 Pütter-type model, which is the result of two antagonistic allometric processes, biomass gains  
 456 and biomass losses:  
 457 
$$\frac{dM}{dt} = H(T)M^a - K(T)M^b \quad (7)$$
  
 458 where  $M$  is body mass and  $T$  is temperature,  $H$  and  $K$  the allometric constants and  $a$  and  $b$  the  
 459 exponents of the processes underlying gains and losses, respectively. We convert metabolism  
 460 from oxygen consumption [ $\text{mg O}_2 \text{ h}^{-1} \text{ day}^{-1}$ ] to  $\text{g day}^{-1}$  by assuming 1 kcal = 295 mg  $\text{O}_2$  (based  
 461 on an oxycaloric coefficient of 14.2 J/mg  $\text{O}_2$ ) (102), 1 kcal = 4184 J and an energy content of 5600  
 462 J/g (103), and convert consumption to  $\text{g day}^{-1}$  from  $\text{g g}^{-1} \text{ day}^{-1}$ . Consumption and metabolic rate  
 463 are calculated for two sizes (5 and 1000 g, which roughly correspond to the 25<sup>th</sup> percentile of both  
 464 datasets and the maximum mass in the consumption data, respectively), using the global  
 465 allometric relationships found in the log-log models fit to sub-peak temperatures. These allometric  
 466 functions are further scaled with the temperature correction factors  $r_c$  for consumption and  $r_m$  for  
 467 metabolism.  $r_c$  is based on the Sharpe-Schoolfield model and  $r_m$  is given by the temperature  
 468 dependence of metabolic rate from the log-linear model. Because  $r_c$  and  $r_m$  are fitted to data on  
 469 different scales, we divide these functions by their maximum. Lastly, we rescale the product  
 470 between the allometric functions and  $r_c$  and  $r_m$  such that the rate at 19°C (mean temperature in  
 471 both data sets) equals the temperature-independent rate.  
 472  
 473  
 474 **Acknowledgments**  
 475 We thank Hiroki Yamanaka, Dennis Tomalá Solano, Vanessa Messmer, Björn Björnsson, Albert  
 476 Imsland, Tomas Árnasson, Yiping Luo, Takeshi Tomiyama and Myron Peck for generously  
 477 providing data; Magnus Huss and Ken Haste Andersen, for providing useful comments on earlier  
 478 versions of the manuscript; Daniel Padfield and Wilco Verberk for helpful discussions; Matthew  
 479 Low and Malin Aronson for an introduction to Bayesian inference. This study was supported by  
 480 grants from the Swedish Research Council FORMAS (no. 217-2013-1315) and the Swedish  
 481 Research Council (no. 2015-03752) (both to AG).  
 482  
 483 **Data accessibility statement**  
 484 All data and R code (lists of studies in literature search, data preparation, analyses and figures)  
 485 can be downloaded from a GitHub repository (<https://github.com/maxlindmark/scaling>) and will be  
 486 archived on Zenodo upon publication.  
 487  
 488  
 489 **References**  
 490 1. J. H. Brown, J. F. Gillooly, A. P. Allen, V. M. Savage, G. B. West, Toward a metabolic  
 491 theory of ecology. *Ecology* **85**, 1771–1789 (2004).  
 492 2. V. M. Savage, J. F. Gillooly, J. H. Brown, G. B. West, E. L. Charnov, Effects of body size  
 493 and temperature on population growth. *The American Naturalist* **163**, 429–441 (2004).

- 494 3. K. H. Andersen, J. E. Beyer, P. Lundberg, Trophic and individual efficiencies of size-  
495 structured communities. *Proceedings of the Royal Society B: Biological Sciences* **276**,  
496 109–114 (2009).
- 497 4. D. R. Barneche, A. P. Allen, The energetics of fish growth and how it constrains food-web  
498 trophic structure. *Ecology Letters* **21**, 836–844 (2018).
- 499 5. M. Daufresne, K. Lengfellner, U. Sommer, Global warming benefits the small in aquatic  
500 ecosystems. *Proceedings of the National Academy of Sciences, USA* **106**, 12788–12793  
501 (2009).
- 502 6. J. L. Gardner, A. Peters, M. R. Kearney, L. Joseph, R. Heinsohn, Declining body size: a  
503 third universal response to warming? *Trends in Ecology & Evolution* **26**, 285–291 (2011).
- 504 7. D. Atkinson, “Temperature and organism size—A biological law for ectotherms?” in  
505 *Advances in Ecological Research*, (Elsevier, 1994), pp. 1–58.
- 506 8. J. Ohlberger, Climate warming and ectotherm body size – from individual physiology to  
507 community ecology. *Functional Ecology* **27**, 991–1001 (2013).
- 508 9. C. R. Horne, Andrew. G. Hirst, D. Atkinson, Temperature-size responses match latitudinal-  
509 size clines in arthropods, revealing critical differences between aquatic and terrestrial  
510 species. *Ecology Letters* **18**, 327–335 (2015).
- 511 10. J. Forster, A. G. Hirst, D. Atkinson, Warming-induced reductions in body size are greater  
512 in aquatic than terrestrial species. *PNAS* **109**, 19310–19314 (2012).
- 513 11. R. E. Thresher, J. A. Koslow, A. K. Morison, D. C. Smith, Depth-mediated reversal of the  
514 effects of climate change on long-term growth rates of exploited marine fish. *Proceedings  
515 of the National Academy of Sciences, USA* **104**, 7461–7465 (2007).
- 516 12. A. B. Neuheimer, R. E. Thresher, J. M. Lyle, J. M. Semmens, Tolerance limit for fish  
517 growth exceeded by warming waters. *Nature Climate Change* **1**, 110–113 (2011).
- 518 13. A. R. Baudron, C. L. Needle, A. D. Rijsdorp, C. T. Marshall, Warming temperatures and  
519 smaller body sizes: synchronous changes in growth of North Sea fishes. *Global Change  
520 Biology* **20**, 1023–1031 (2014).
- 521 14. M. Huss, M. Lindmark, P. Jacobson, R. M. Van Dorst, A. Gårdmark, Experimental  
522 evidence of gradual size-dependent shifts in body size and growth of fish in response to  
523 warming. *Glob Change Biol* **25**, 2285–2295 (2019).
- 524 15. I. E. Ikpewe, A. R. Baudron, A. Ponchon, P. G. Fernandes, Bigger juveniles and smaller  
525 adults: Changes in fish size correlate with warming seas. *Journal of Applied Ecology Early  
526 View* (2020).
- 527 16. I. van Rijn, Y. Buba, J. DeLong, M. Kiflawi, J. Belmaker, Large but uneven reduction in fish  
528 size across species in relation to changing sea temperatures. *Global Change Biology* **23**,  
529 3667–3674 (2017).
- 530 17. D. R. Barneche, M. Jahn, F. Seebacher, Warming increases the cost of growth in a model  
531 vertebrate. *Functional Ecology* **33**, 1256–1266 (2019).
- 532 18. R. M. Van Dorst, et al., Warmer and browner waters decrease fish biomass production.  
533 *Global Change Biology* **25**, 1395–1408 (2019).
- 534 19. A. Audzijonyte, et al., Fish body sizes change with temperature but not all species shrink  
535 with warming. *Nat Ecol Evol* **4**, 809–814 (2020).
- 536 20. D. van Denderen, H. Gislason, J. van den Heuvel, K. H. Andersen, Global analysis of fish  
537 growth rates shows weaker responses to temperature than metabolic predictions. *Global  
538 Ecology and Biogeography* **29**, 2203–2213 (2020).
- 539 21. H.-Y. Wang, S.-F. Shen, Y.-S. Chen, Y.-K. Kiang, M. Heino, Life histories determine  
540 divergent population trends for fishes under climate warming. *Nature Communications* **11**,  
541 4088 (2020).
- 542 22. A. Audzijonyte, et al., Is oxygen limitation in warming waters a valid mechanism to explain  
543 decreased body sizes in aquatic ectotherms? *Global Ecology and Biogeography* **28**, 64–  
544 77 (2019).
- 545 23. P. Neubauer, K. H. Andersen, Thermal performance of fish is explained by an interplay  
546 between physiology, behaviour and ecology. *Conserv Physiol* **7** (2019).

- 547 24. A. Pütter, Studien über physiologische Ähnlichkeit VI. Wachstumsähnlichkeiten. *Pflügers  
548 Arch.* **180**, 298–340 (1920).
- 549 25. L. von Bertalanffy, Laws in metabolism and growth. *The quarterly review of biology* **32**,  
550 217–231 (1957).
- 551 26. K. Morita, M. Fukuwaka, N. Tanimata, O. Yamamura, Size-dependent thermal preferences  
552 in a pelagic fish. *Oikos* **119**, 1265–1272 (2010).
- 553 27. D. Pauly, W. W. L. Cheung, Sound physiological knowledge and principles in modeling  
554 shrinking of fishes under climate change. *Global Change Biology* **24**, e15–e26 (2018).
- 555 28. D. Pauly, The gill-oxygen limitation theory (GOLT) and its critics. *Science Advances* **7**,  
556 eabc6050 (2021).
- 557 29. S. Lefevre, D. J. McKenzie, G. E. Nilsson, In modelling effects of global warming, invalid  
558 assumptions lead to unrealistic projections. *Global Change Biology* **24**, 553–556 (2018).
- 559 30. D. J. Marshall, C. R. White, Have we outgrown the existing models of growth? *Trends in  
560 Ecology & Evolution* **34**, 102–111 (2019).
- 561 31. E. Ursin, A Mathematical Model of Some Aspects of Fish Growth, Respiration, and  
562 Mortality. *Journal of the Fisheries Research Board of Canada* **24**, 2355–2453 (1967).
- 563 32. J. F. Kitchell, D. J. Stewart, D. Weininger, Applications of a bioenergetics model to yellow  
564 perch (*Perca flavescens*) and walleye (*Stizostedion vitreum vitreum*). *Journal of the  
565 Fisheries Board of Canada* **34**, 1922–1935 (1977).
- 566 33. M. Jobling, “Temperature and growth: modulation of growth rate via temperature change”  
567 in *Global Warming: Implications for Freshwater and Marine Fish*, C. M. Wood, D. G.  
568 McDonald, Eds. (Cambridge University Press, 1997), pp. 225–254.
- 569 34. T. E. Essington, J. F. Kitchell, C. J. Walters, The von Bertalanffy growth function,  
570 bioenergetics, and the consumption rates of fish. *Canadian Journal of Fisheries and  
571 Aquatic Sciences* **58**, 2129–2138 (2001).
- 572 35. S. A. L. M. Kooijman, *Dynamic energy budgets in biological systems* (Cambridge  
573 University Press, 1993).
- 574 36. A. M. de Roos, L. Persson, Physiologically structured models – from versatile technique to  
575 ecological theory. *Oikos* **94**, 51–71 (2001).
- 576 37. M. Hartvig, K. H. Andersen, J. E. Beyer, Food web framework for size-structured  
577 populations. *Journal of Theoretical Biology* **272**, 113–122 (2011).
- 578 38. O. Maury, J.-C. Poggiale, From individuals to populations to communities: A dynamic  
579 energy budget model of marine ecosystem size-spectrum including life history diversity.  
580 *Journal of Theoretical Biology* **324**, 52–71 (2013).
- 581 39. J. L. Blanchard, R. F. Heneghan, J. D. Everett, R. Trebilco, A. J. Richardson, From  
582 bacteria towWhales: Using functional size spectra to model marine ecosystems. *Trends in  
583 Ecology & Evolution* **32**, 174–186 (2017).
- 584 40. D. S. Glazier, Beyond the “3/4-power law”: variation in the intra- and interspecific scaling of  
585 metabolic rate in animals. *Biological Reviews of the Cambridge Philosophical Society* **80**,  
586 611–662 (2005).
- 587 41. B. C. Rall, *et al.*, Universal temperature and body-mass scaling of feeding rates.  
588 *Philosophical Transactions of the Royal Society of London, Series B: Biological Sciences*  
589 **367**, 2923–2934 (2012).
- 590 42. C. L. Jerde, *et al.*, Strong Evidence for an Intraspecific Metabolic Scaling Coefficient Near  
591 0.89 in Fish. *Front. Physiol.* **10**, 1166 (2019).
- 592 43. J. F. Gillooly, J. H. Brown, G. B. West, V. M. Savage, E. L. Charnov, Effects of size and  
593 temperature on metabolic rate. *Science*, 2248–2251. (2001).
- 594 44. C. J. Downs, J. P. Hayes, C. R. Tracy, Scaling metabolic rate with body mass and inverse  
595 body temperature: A test of the Arrhenius fractal supply model. *Functional Ecology* **22**,  
596 239–244 (2008).
- 597 45. A. Clarke, N. M. Johnston, Scaling of metabolic rate with body mass and temperature in  
598 teleost fish. *Journal of Animal Ecology* **68**, 893–905 (1999).
- 599 46. F. Bokma, Evidence against universal metabolic allometry. *Functional Ecology* **18**, 184–  
600 187 (2004).

- 601 47. A. I. Dell, S. Pawar, V. M. Savage, Systematic variation in the temperature dependence of  
602 physiological and ecological traits. *Proceedings of the National Academy of Sciences* **108**,  
603 10591–10596 (2011).
- 604 48. G. Englund, G. Öhlund, C. L. Hein, S. Diehl, Temperature dependence of the functional  
605 response. *Ecology Letters* **14**, 914–921 (2011).
- 606 49. S. F. Uiterwaal, J. P. DeLong, Functional responses are maximized at intermediate  
607 temperatures. *Ecology* **101**, e02975 (2020).
- 608 50. Xiaojun. Xie, Ruyung. Sun, The Bioenergetics of the Southern Catfish (*Silurus meridionalis*  
609 Chen). I. Resting Metabolic Rate as a Function of Body Weight and Temperature.  
610 *Physiological Zoology* **63**, 1181–1195 (1990).
- 611 51. B. García García, J. Cerezo Valverde, F. Aguado-Giménez, J. García García, M. D.  
612 Hernández, Effect of the interaction between body weight and temperature on growth and  
613 maximum daily food intake in sharpsnout sea bream (*Diplodus puntazzo*). *Aquaculture  
614 International* **19**, 131–141 (2011).
- 615 52. J. Ohlberger, Thomas. Mehner, Georg. Staaks, Franz. Hölker, Intraspecific temperature  
616 dependence of the scaling of metabolic rate with body mass in fishes and its ecological  
617 implications. *Oikos* **121**, 245–251 (2012).
- 618 53. M. Lindmark, M. Huss, J. Ohlberger, A. Gårdmark, Temperature-dependent body size  
619 effects determine population responses to climate warming. *Ecology Letters* **21**, 181–189  
620 (2018).
- 621 54. R. M. Schoolfield, P. J. H. Sharpe, C. E. Magnuson, Non-linear regression of biological  
622 temperature-dependent rate models based on absolute reaction-rate theory. *Journal of  
623 Theoretical Biology* **88**, 719–731 (1981).
- 624 55. D. Pauly, W. W. L. Cheung, On confusing cause and effect in the oxygen limitation of fish.  
625 *Global Change Biology* **24**, e743–e744 (2018).
- 626 56. N. P. Lemoine, D. E. Burkepile, Temperature-induced mismatches between consumption  
627 and metabolism reduce consumer fitness. *Ecology* **93**, 2483–2489 (2012).
- 628 57. B. C. Rall, O. Vucic-Pestic, R. B. Ehnes, M. Emmerson, U. Brose, Temperature, predator–  
629 prey interaction strength and population stability. *Global Change Biology* **16**, 2145–2157  
630 (2010).
- 631 58. M. J. Angilletta, A. E. Dunham, The temperature-size rule in ectotherms: simple  
632 evolutionary explanations may not be general. *The American Naturalist* **162**, 332–342  
633 (2003).
- 634 59. D. A. Vasseur, K. S. McCann, A mechanistic approach for modelling temperature-  
635 dependent consumer-resource dynamics. *The American Naturalist* **166**, 184–198 (2005).
- 636 60. K. E. Fussmann, F. Schwarzmüller, U. Brose, A. Jousset, B. C. Rall, Ecological stability in  
637 response to warming. *Nature Climate Change* **4**, 206–210 (2014).
- 638 61. M. Lindmark, J. Ohlberger, M. Huss, A. Gårdmark, Size-based ecological interactions  
639 drive food web responses to climate warming. *Ecology Letters* **22**, 778–786 (2019).
- 640 62. J. Wyban, W. A. Walsh, D. M. Godin, Temperature effects on growth, feeding rate and  
641 feed conversion of the Pacific white shrimp (*Penaeus vannamei*). *Aquaculture* **138**, 267–  
642 279 (1995).
- 643 63. V. E. Panov, D. J. McQueen, Effects of temperature on individual growth rate and body  
644 size of a freshwater amphipod. **76**, 1107–1116 (1998).
- 645 64. A. Steinarsson, A. K. Imsland, Size dependent variation in optimum growth temperature of  
646 red abalone (*Haliotis rufescens*). *Aquaculture* **224**, 353–362 (2003).
- 647 65. B. Björnsson, A. Steinarsson, T. Árnason, Growth model for Atlantic cod (*Gadus morhua*):  
648 Effects of temperature and body weight on growth rate. *Aquaculture* **271**, 216–226 (2007).
- 649 66. S. O. Handeland, A. K. Imsland, S. O. Stefansson, The effect of temperature and fish size  
650 on growth, feed intake, food conversion efficiency and stomach evacuation rate of Atlantic  
651 salmon post-smolts. *Aquaculture* **283**, 36–42 (2008).
- 652 67. J. R. Brett, J. E. Shelbourn, C. T. Shoop, Growth rate and body composition of fingerling  
653 sockeye salmon, *Oncorhynchus nerka*, in relation to temperature and ration size. *J. Fish.  
654 Res. Bd. Can.* **26**, 2363–2394 (1969).

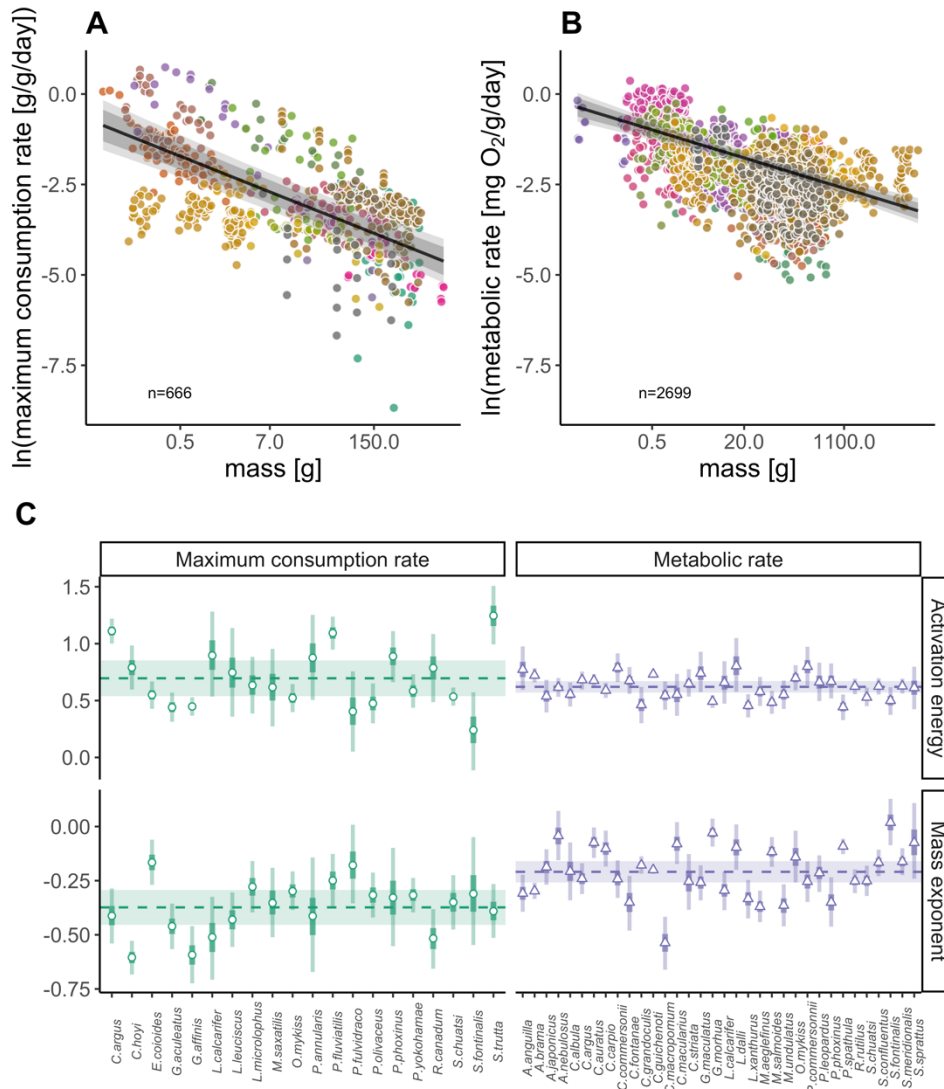
- 655 68. J. M. Elliott, M. A. Hurley, The functional relationship between body size and growth rate in  
656 fish. *Functional Ecology* **9**, 625 (1995).
- 657 69. D. R. Barneche, D. R. Robertson, C. R. White, D. J. Marshall, Fish reproductive-energy  
658 output increases disproportionately with body size. *Science* **360**, 642–645 (2018).
- 659 70. K. Lorenzen, The relationship between body weight and natural mortality in juvenile and  
660 adult fish: a comparison of natural ecosystems and aquaculture. *Journal of Fish Biology*  
661 **49**, 627–642 (1996).
- 662 71. R. B. Huey, J. G. Kingsolver, Climate warming, resource availability, and the metabolic  
663 meltdown of ectotherms. *The American Naturalist* **194**, E140–E150 (2019).
- 664 72. S. Neuenfeldt, *et al.*, Feeding and growth of Atlantic cod (*Gadus morhua* L.) in the eastern  
665 Baltic Sea under environmental change. *ICES Journal of Marine Science* **77**, 624–632  
666 (2020).
- 667 73. J. Ohlberger, E. Edeline, L. A. Vollestad, N. C. Stenseth, D. Claessen, Temperature-driven  
668 regime shifts in the dynamics of size-structured populations. *The American Naturalist* **177**,  
669 211–223 (2011).
- 670 74. J. R. Brett, Energetic responses of salmon to temperature. A study of some thermal  
671 relations in the physiology and freshwater ecology of sockeye salmon (*Oncorhynchus*  
672 *nerka*). *Integr Comp Biol* **11**, 99–113 (1971).
- 673 75. E. E. Werner, D. J. Hall, Ontogenetic habitat shifts in bluegill: The foraging rate-predation  
674 risk trade-off. *Ecology* **69**, 1352–1366 (1988).
- 675 76. E. Lloret-Lloret, *et al.*, The seasonal distribution of a highly commercial fish is related to  
676 ontogenetic changes in its feeding strategy. *Front. Mar. Sci.* **7** (2020).
- 677 77. Heincke F., Rapp. Proc. Verb. Réun. ICES 16, 1–70. (1913).
- 678 78. A. Audzijonyte, G. T. Pecl, Deep impact of fisheries. *Nature Ecology & Evolution* **2**, 1348–  
679 1349 (2018).
- 680 79. H. O. Pörtner, R. Knust, Climate change affects marine fishes through the oxygen  
681 limitation of thermal tolerance. *Science* **315**, 95–97 (2007).
- 682 80. W. W. L. Cheung, *et al.*, Shrinking of fishes exacerbates impacts of global ocean changes  
683 on marine ecosystems. *Nature Climate Change* **3**, 254–258 (2013).
- 684 81. B. Gilbert, *et al.*, A bioenergetic framework for the temperature dependence of trophic  
685 interactions. *Ecology Letters* **17**, 902–914 (2014).
- 686 82. J. A. Nelson, Oxygen consumption rate v. rate of energy utilization of fishes: a comparison  
687 and brief history of the two measurements. *Journal of Fish Biology* **88**, 10–25 (2016).
- 688 83. J. D. Armstrong, L. A. Hawkins, Standard metabolic rate of pike, *Esox lucius*: variation  
689 among studies and implications for energy flow modelling. *Hydrobiologia* **601**, 83–90  
690 (2008).
- 691 84. A. Rohatgi, *WebPlotDigitalizer: HTML5 based online tool to extract numerical data from*  
692 *plot images. Version 4.1. [WWW document] URL* <https://automeris.io/WebPlotDigitizer>  
693 *(accessed on January 2019).* (2012).
- 694 85. A. Gelman, J. Hill, *Data Analysis Using Regression and Multilevel/Hierarchical Models*  
695 (Cambridge University Press, 2007).
- 696 86. X. A. Harrison, *et al.*, A brief introduction to mixed effects modelling and multi-model  
697 inference in ecology. *PeerJ* **6**, e4794 (2018).
- 698 87. H. Schielzeth, Simple means to improve the interpretability of regression coefficients:  
699 Interpretation of regression coefficients. *Methods in Ecology and Evolution* **1**, 103–113  
700 (2010).
- 701 88. F. W. H. Beamish, Respiration of fishes with special emphasis on standard oxygen  
702 consumption II. Influence of weight and temperature on respiration of several species'.  
703 *Canadian Journal of Zoology/Revue Canadienne de Zoologie* **42**, 177–188 (1964).
- 704 89. J. Ohlberger, G. Staaks, F. Höller, Effects of temperature, swimming speed and body  
705 mass on standard and active metabolic rate in vendace (*Coregonus albula*). *Journal of*  
706 *Comparative Physiology, B* **177**, 905–916 (2007).

- 707 90. D. Padfield, M. Castledine, A. Buckling, Temperature-dependent changes to host–parasite  
708 interactions alter the thermal performance of a bacterial host. *The ISME Journal* **14**, 389–  
709 398 (2020).
- 710 91. R Core Team, *R: A Language and Environment for Statistical Computing*. R Foundation  
711 for Statistical Computing (2020).
- 712 92. M. Plummer, JAGS: A program for analysis of Bayesian graphical models using Gibbs  
713 sampling. *Working Papers*, 8 (2003).
- 714 93. M. Plummer, *rjags* (2019).
- 715 94. A. Gelman, J. Carlin, H. Stern, D. Rubin, *Bayesian Data Analysis. 2nd edition* (Chapman  
716 and Hall/CRC, 2003).
- 717 95. H. Wickham, *et al.*, Welcome to the tidyverse. *Journal of Open Source Software*, 1686  
718 (2019).
- 719 96. X. Fernández-i-Marín, ggmcmc: Analysis of MCMC Samples and Bayesian Inference.  
720 *Journal of Statistical Software* **70**, 1–20 (2016).
- 721 97. C. Youngflesh, MCMCvis: Tools to Visualize, Manipulate, and Summarize MCMC Output.  
722 *Journal of Open Source Software* **3**, 640 (2018).
- 723 98. J. Gabry, D. Simpson, A. Vehtari, M. Betancourt, A. Gelman, Visualization in Bayesian  
724 workflow. *J. R. Stat. Soc. A* **182**, 389–402 (2019).
- 725 99. S. Watanabe, A Widely Applicable Bayesian Information Criterion. *Journal of Machine  
726 Learning Research* **14**, 867–897 (2013).
- 727 100. A. Vehtari, A. Gelman, J. Gabry, Practical Bayesian model evaluation using leave-one-out  
728 cross-validation and WAIC. *Stat Comput* **27**, 1413–1432 (2017).
- 729 101. M. Olmos, *et al.*, Spatial synchrony in the response of a long range migratory species  
730 (*Salmo salar*) to climate change in the North Atlantic Ocean. *Global Change Biology* **26**,  
731 1319–1337 (2019).
- 732 102. B. Hepher, *Nutrition of Pond Fishes* (Cambridge University Press, 1988).
- 733 103. A. D. Rijnsdorp, B. Ibelings, Sexual dimorphism in the energetics of reproduction and  
734 growth of North Sea plaice, *Pleuronectes platessa* L. *Journal of Fish Biology* **35**, 401–415  
735 (1989).

736

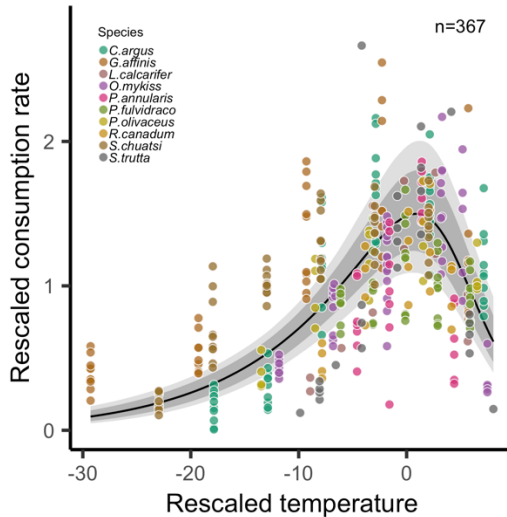
737  
738  
739

## Figures and Tables



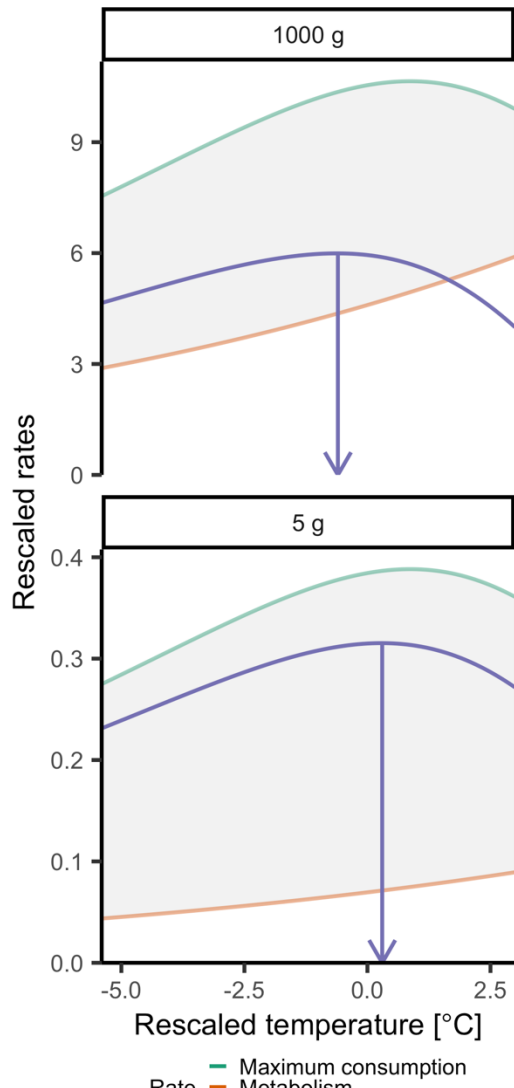
740  
741  
742  
743  
744  
745  
746  
747  
748  
749  
750  
751  
752  
753

**Figure 1.** Natural log of mass-specific maximum consumption rate (A) and metabolic rate (B) against body mass on a logarithmic x-axis. Lines are global predictions at the average temperature in each data set (both 19°C, but note the model is fitted using mean-centred Arrhenius temperature). Shaded areas correspond to 80% and 95% credible intervals. Species are grouped by color (legend not shown, n=20 for consumption and n=34 for metabolism, respectively). C) Global and species-level effects of mass- and temperature on specific maximum consumption rate and metabolic rate. Horizontal lines show the posterior medians of the global activation energies and mass exponents of maximum consumption and metabolism ( $\mu_{\beta_1}$  and  $\mu_{\beta_2}$  in Eqs. 6-8 for the mass and temperature coefficients, respectively). The shaded horizontal rectangles correspond to the posterior median  $\pm 2$  standard deviations. Points and triangles show the posterior medians for each species-level coefficient (for maximum consumption rate and metabolic rate, respectively), and the vertical bars show their 80% and 95% credible interval.

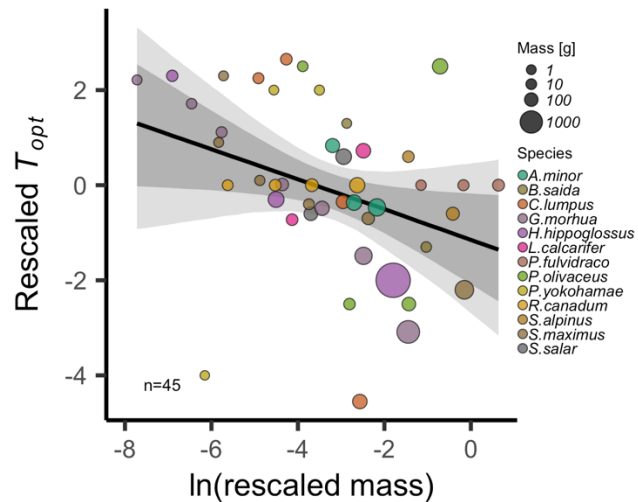


754  
755  
756  
757  
758  
759  
760  
761  
762  
763

**Figure 2.** Mass-specific maximum consumption rate increases until a maximum is reached, after which it declines steeper than the initial rate of increase. Maximum consumption rates are relative to the average maximum consumption rates within species and temperature is the difference between the experimental temperature and the temperature where maximum consumption peaks (also by species). Lines show posterior median of predictions from the Sharpe-Schoolfield model (using the average intercept across species and the common coefficients), grey bands show 95% and 80% credible intervals. Colors indicate species.



764  
 765 **Figure 3.** Illustration of predicted whole-organism maximum consumption rate (green), metabolic  
 766 rate (purple) and the difference between them (orange) for two body sizes (top=1000g,  
 767 bottom=5g) (see 'Materials and Methods'). Vertical arrows indicate the temperature where the  
 768 difference in net energy gain (energy available for growth) is maximized for the two body sizes,  
 769 which occurs at different temperatures despite that consumption peaks at the same temperature  
 770 for both body sizes.  
 771



772  
 773 **Figure 4.** Experimental data demonstrating optimum growth temperature declines with body  
 774 mass. The plot shows the optimum temperature within species (rescaled by subtracting the mean  
 775 optimum temperature from each observation, by species) as a function of the natural log of  
 776 rescaled body mass (ratio of mass to maturation mass within species). Probability bands  
 777 represent 80% and 95% credible intervals, and the solid line shows the global prediction ( $\mu_{\beta_0}$  and  
 778  $\mu_{\beta_1}$ ). Colors indicate species and the area of the circle corresponds to body mass in unit g.  
 779



**Supplementary Information for**  
Optimum growth temperature declines with body size within fish  
species

Max Lindmark<sup>a,1</sup>, Jan Ohlberger<sup>b</sup>, Anna Gårdmark<sup>c</sup>

Max Lindmark, Swedish University of Agricultural Sciences, Department of Aquatic Resources,  
Institute of Marine Research, Turistgatan 5, Lysekil 453 30, Sweden, Tel.: +46(0)104784137  
Email: [max.lindmark@slu.se](mailto:max.lindmark@slu.se)

**This PDF file includes:**

Supplementary text  
Figures S1 to S27  
Tables S1 to S5  
SI References

## **Supplementary Information Text**

### **Literature search, selection process and criteria**

This section is an overview of the literature search approach, and below we present the search terms for each rate separately (maximum consumption, metabolism and growth). In addition to search terms, we also applied filters by selecting only the following subjects: ‘marine freshwater biology’, ‘fisheries’, ‘ecology’, ‘zoology’, ‘biology’, ‘physiology’. For growth rates, we also included ‘limnology’ and for maximum consumption we included ‘limnology’ and ‘evolutionary biology’. The use of additional subjects for growth and consumption reflects the lower data availability compared to metabolism. As we suspected that relatively few studies would have considered both body size- and temperature treatments, our goal was to get an as extensive as possible list of studies. Therefore, we also evaluated articles cited by articles found in the search, from published review-type articles and reviews of applications of bioenergetics models such as the Wisconsin model (1), and if the study was found in the literature search for another rate. The source of the article (WoS search or cited in literature) is indicated in the data sets (Table S1).

Articles were filtered out at three levels of the search: title, abstract and full article. The online repository of this project (<https://github.com/maxlindmark/scaling>) contains .txt files of the complete list of articles found in the literature search. We removed studies from the lists if the titles made it clear the articles did not fulfil all of the following conditions: (1) experimental study, (2) fish as study organism in post-larval life stages, and (3) replicates across both body size and temperature (factorially). We treat data as individual-level rates (per fish); however, in some cases they were measured as averages across multiple individuals. In addition to these general criteria, we also had criteria specific for each rate (see below). When several studies were found for the same species, we did not include all but instead chose the study with the largest body size and temperature range (in that order), as there can be large differences in absolute values of some physiological parameters between studies.

For consumption and growth rate, we determined if each data point within species was below or beyond peak temperature either by using information provided by the authors (e.g. by deriving a polynomial regression of the rate as a function of temperature to find the temperature of peak rate), by fitting quadratic models or visually inspecting data for each species separately. Whether a data point was below or above peak or optimum temperatures is indicated by a separate column in the data (Table S1).

### **Maximum consumption rate**

We used the following topic terms for maximum consumption rate (three searches in total): (consumption OR bioenerg\* OR ingestion OR “food-intake”) AND (mass OR weight OR size) AND (temperature\*), as well as: (feeding-rate OR bio-energ\*) AND (mass OR weight OR size) AND (temperature\*) and lastly: (“food intake”) AND (mass OR weight OR size) AND (temperature\*). \* represents any group of characters, including no character. The searches for maximum consumption rate data resulted in 15259 articles (search date: 18 December 2018), with 3449 remaining after filtering by subject categories. The second search (search date: 13 March 2019) resulted in 431 additional titles after filtering by subject categories (of which some were duplicated from the first search) and the third search (search date: 29 June 2020) yielded 626 but no additional articles as they had either been selected already or did not meet the criteria. Articles were filtered out at the abstract and whole article stage if the original reference could not be identified and evaluated, if data were normalized (i.e., using a priori defined scaling relationships to show corrected data rather than measured values), there was no acclimation, or if measurements were not maximum consumption rate. As with the growth data, definitions of ad-libitum feeding may differ between studies – the key for our purpose is that food rations led to satiation and were not limiting. Consumption rates were converted to g day<sup>-1</sup> (but note we fitted models to mass-specific rates, g g<sup>-1</sup> day<sup>-1</sup>). These data were compiled in the file consumption\_data.xlsx.

### **Metabolic rate**

We used the following topic terms for metabolic rate data: (metabolism OR "oxygen-consumption" OR "oxygen consumption") AND (mass OR weight OR size) AND (temperature\*). \* represents any group of characters, including no character. The search for metabolic rate experiments resulted in 8405 articles (search date: 6 June 2019), which was reduced to 3458 after applying filters for subject categories. Articles were filtered out at the abstract and whole article stage if the original reference could not be identified and evaluated, if data were normalized (i.e., using a priori defined scaling relationships to normalize data for data a given size rather than measured values), if there was no acclimation or if it was not standard, routine or resting metabolic rate. The latter was defined as oxygen consumption of an unfed fish at no or little spontaneous activity. Metabolic rates were converted to mg O<sub>2</sub> h<sup>-1</sup>, because it was the most common unit in the data set (but note models were fitted to mass-specific rates, mg O<sub>2</sub> g<sup>-1</sup> h<sup>-1</sup>). These data were compiled in the file metabolism\_data.xlsx.

### **Growth rates & optimum temperature for growth over body mass**

Growth rates were taken from data found in the literature search for optimum growth temperatures. Therefore, articles in which growth rates were measured at sub-optimum temperatures only were not included (note this is in contrast to consumption data where "optimum" was not included in the search terms). We used the following topic terms for growth rate data: (growth) AND (mass OR weight OR size) AND (temperature\*) AND (optimum), as well as: (growth) AND (mass OR weight OR size) AND (temperature\*) AND (optim\*). \* represents any group of characters, including no character. The two searches for growth rates resulted in 3313 articles (search date: 22 March 2019), and 3747 articles (search date: 5 May 2019), respectively. After applying additional filters by subject category, we acquired 566 and 893 studies, respectively (of which some are duplicates due to similar search-strings). We removed studies at the abstract and whole article stage where the original reference could not be identified and evaluated, if we could not extract actual growth rates, if there was not a controlled temperature for each growth trial, or if there were not multiple defined size-classes. We used only one observation (data point) per size class and temperature treatment, and in cases where there were two, we used the mean value. In addition, we ensured that no other treatment (e.g., food limitation) confounded the response variable and thus only used data from experiments with satiating food levels. Body mass is either the geometric mean of the initial and final mass of the growth trial or the size class, depending on data availability (see Table S1). It is important to control for feeding ratios as it affects the temperature optimum for growth (2). This was achieved in different ways in the different experimental studies, but commonly involved excess feeding ratios once or several times per day. The key description we looked for in the study was that food was not limiting. We treat data as individual-level growth (per fish); however, these were commonly measured as averages for multiple individuals. In the case growth was length-based, we converted it to mass using weight-length relationships from FishBase (3, 4). We compiled two separate data sets: raw growth rates (growth\_data.xlsx) and temperature at optimum growth (growth\_data\_Topt.xlsx). In the latter, we defined optimum temperature for growth as the fitted optimum temperature by size-class (usually estimated in the original study). Therefore, the optimum temperature may not always correspond to an actual experimental temperature but could be an estimation. If the optimum temperature (by size group) was not estimated in the original study, we used the temperature where growth rate was maximized. All growth rates were expressed in unit % day<sup>-1</sup>.

### **Supplementary methods and analysis**

At below peak temperatures, the intraspecific mass- and temperature dependence of specific growth (% increase in size day<sup>-1</sup>) can be described by the equation:  $\ln(G) = 0.5 - 0.36 \times \ln(m) - 0.74 \times t_A + 0.0046 \times t_A \times \ln(m)$  (Fig. S12), based on posterior medians of the global parameters, thus representing an average (unmeasured) fish. (see SI Appendix Fig S15, S19, S23 and S27 for the full posteriors distributions of parameters for all models). The mass exponent of growth is estimated to be -0.36 [-0.5, -0.23] and the activation energy ( $-\mu_{\beta_2}$ ) of growth 0.74 [0.95, 0.53]. This is similar to the predicted mass scaling of net energy at sub-optimum temperatures, defined

as the difference between consumption and metabolism (Fig. 3; see also methods on 'Net energy gain'), which scales with a mass-specific exponent of -0.38. The estimated temperature-mass interaction coefficient is both small and uncertain (0.0046 [-0.064, 0.075]), where Bayesian 95% credible intervals are indicated in square brackets.

### Model validation and fit

Figures showing convergence of species-level parameters can be found on:  
<https://github.com/maxlindmark/scaling>, in this section only global parameters are visualized (Fig. S8-S27).

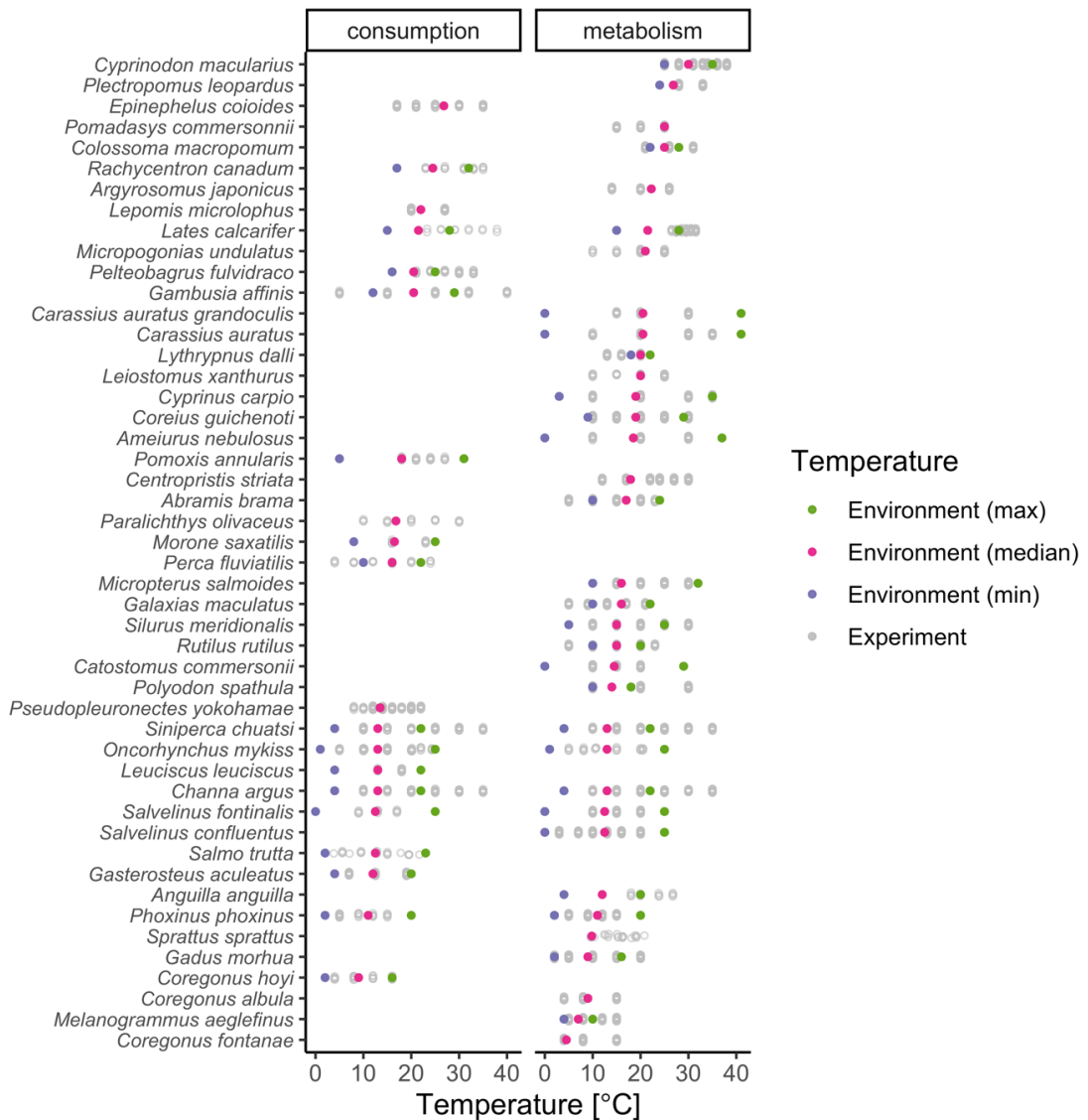


**Fig. S1.** Experimental temperatures (gray) and environmental (min, median and max) temperatures (purple, pink and green, respectively) of species represented in the consumption (left) and metabolism (right) data sets. Missing temperatures means information was not available on FishBase. Experimental temperatures are jittered vertically for visibility.

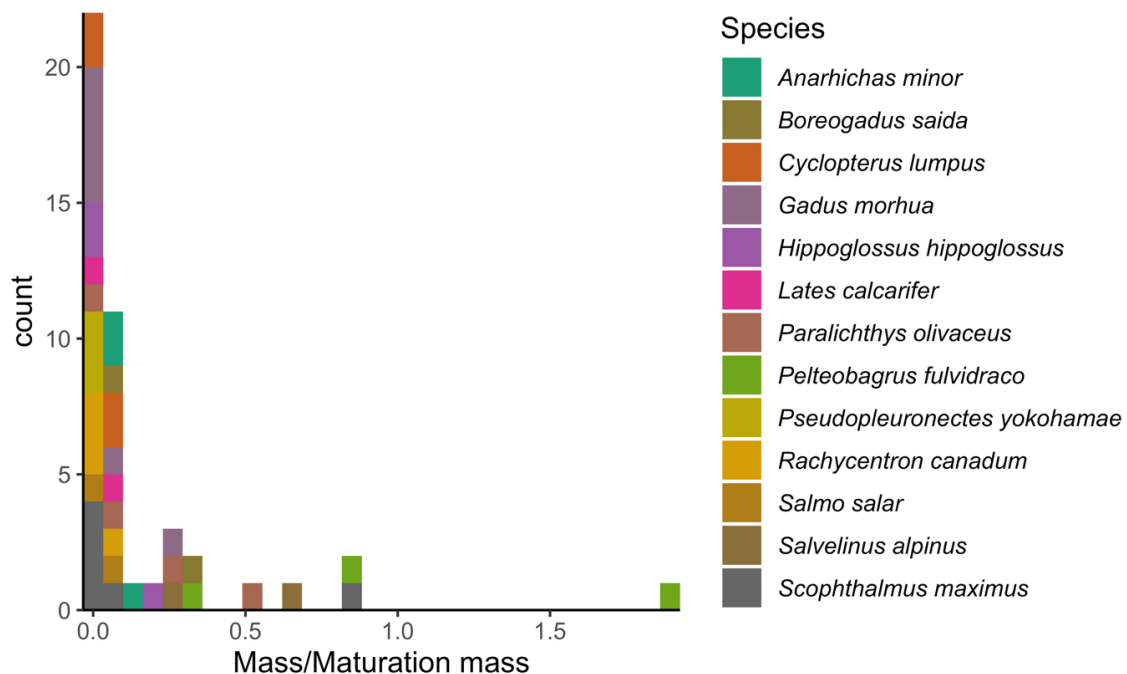


**Fig. S2.** The distribution of rescaled masses for individual observations (mass/mass at maturation), where color indicate species.

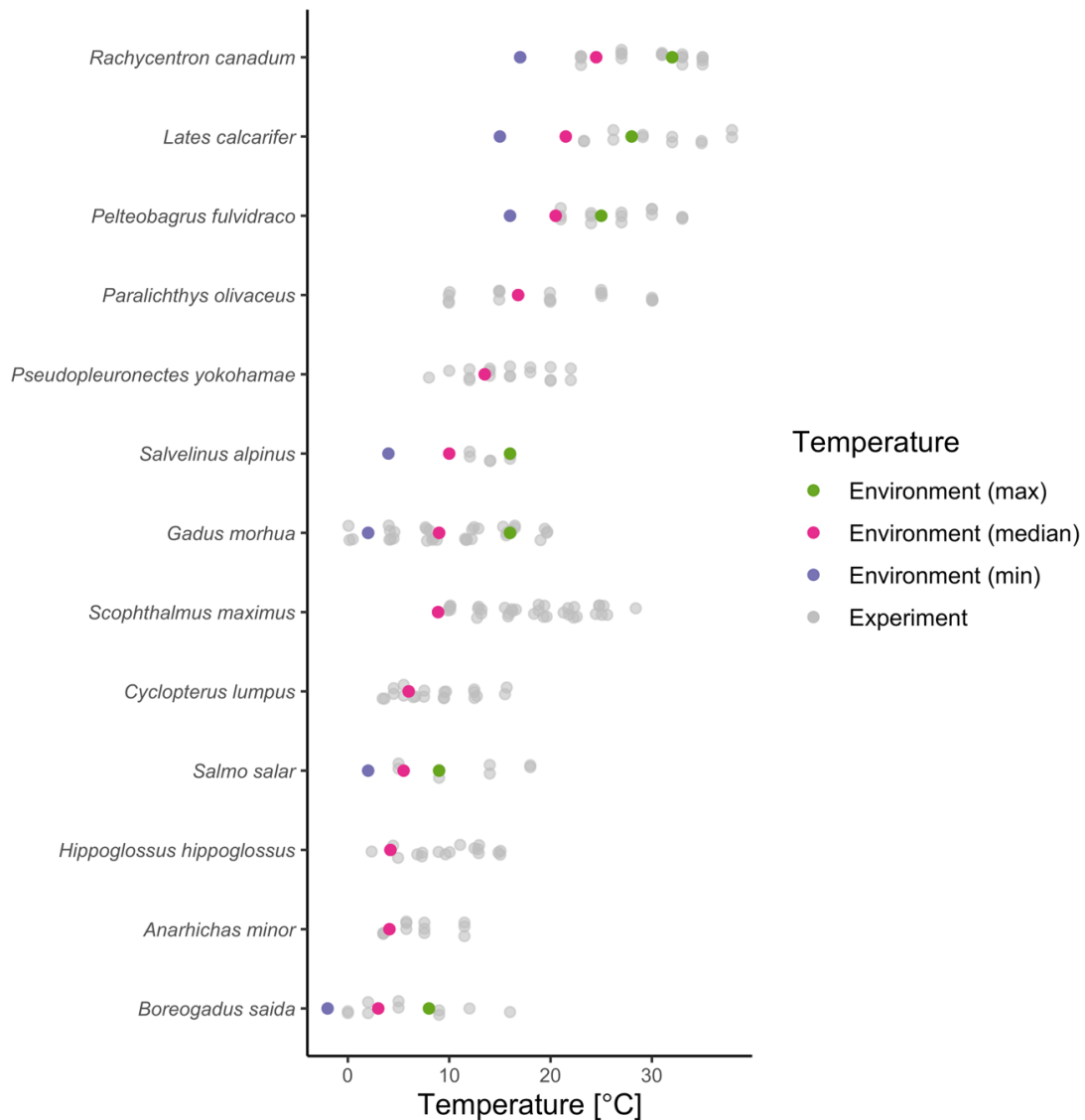


**Fig. S3.** Experimental temperatures (gray) in the growth rate data and environmental (min, median and max) temperatures (purple, pink and green, respectively). Missing temperatures means information was not available on FishBase. Experimental temperatures are jittered vertically for visibility.

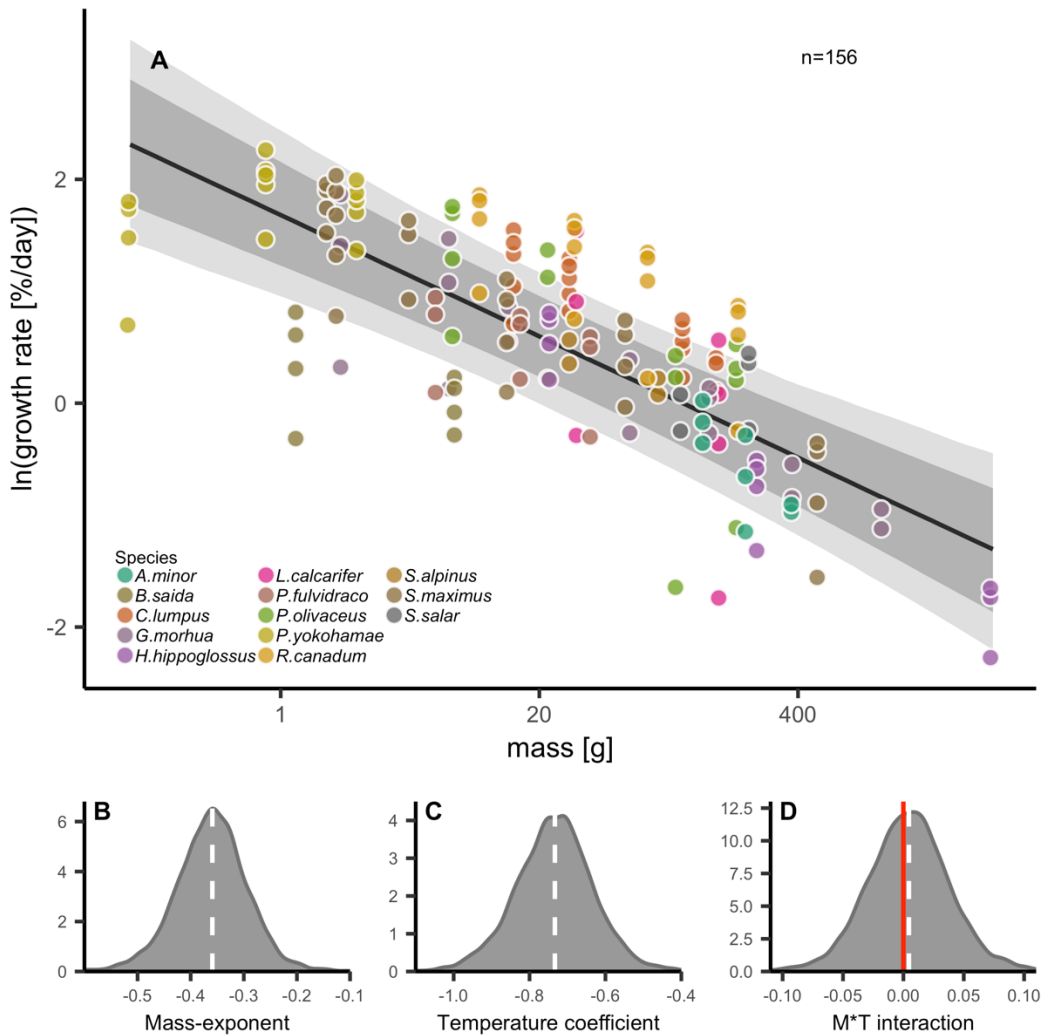


**Fig. S4.** Effects of temperature and body mass on body growth below optimum temperature. Panel A) shows the natural log of specific growth rate as a function of body mass on a logarithmic x-axis (for readability, note the model is fitted with  $\ln(\text{mass})$  as a predictor), such that the slope corresponds to the mass-scaling exponent. Colors indicate species. The line in panel A is the global prediction from model M1 at the mean temperature in the growth data ( $14^{\circ}\text{C}$ , but note the model is fitted using Arrhenius temperature). Shaded areas correspond to 80% and 95% credible intervals. Point colors indicate species. The bottom row shows the posterior distributions for (B) the global mass-scaling exponent,  $\mu_{\beta_1}$ , (C) the global temperature coefficient,  $\mu_{\beta_2}$  and (D) the global mass-temperature interaction,  $\mu_{\beta_3}$ . Dashed white line shows the posterior median and red vertical line in (D) indicates zero.

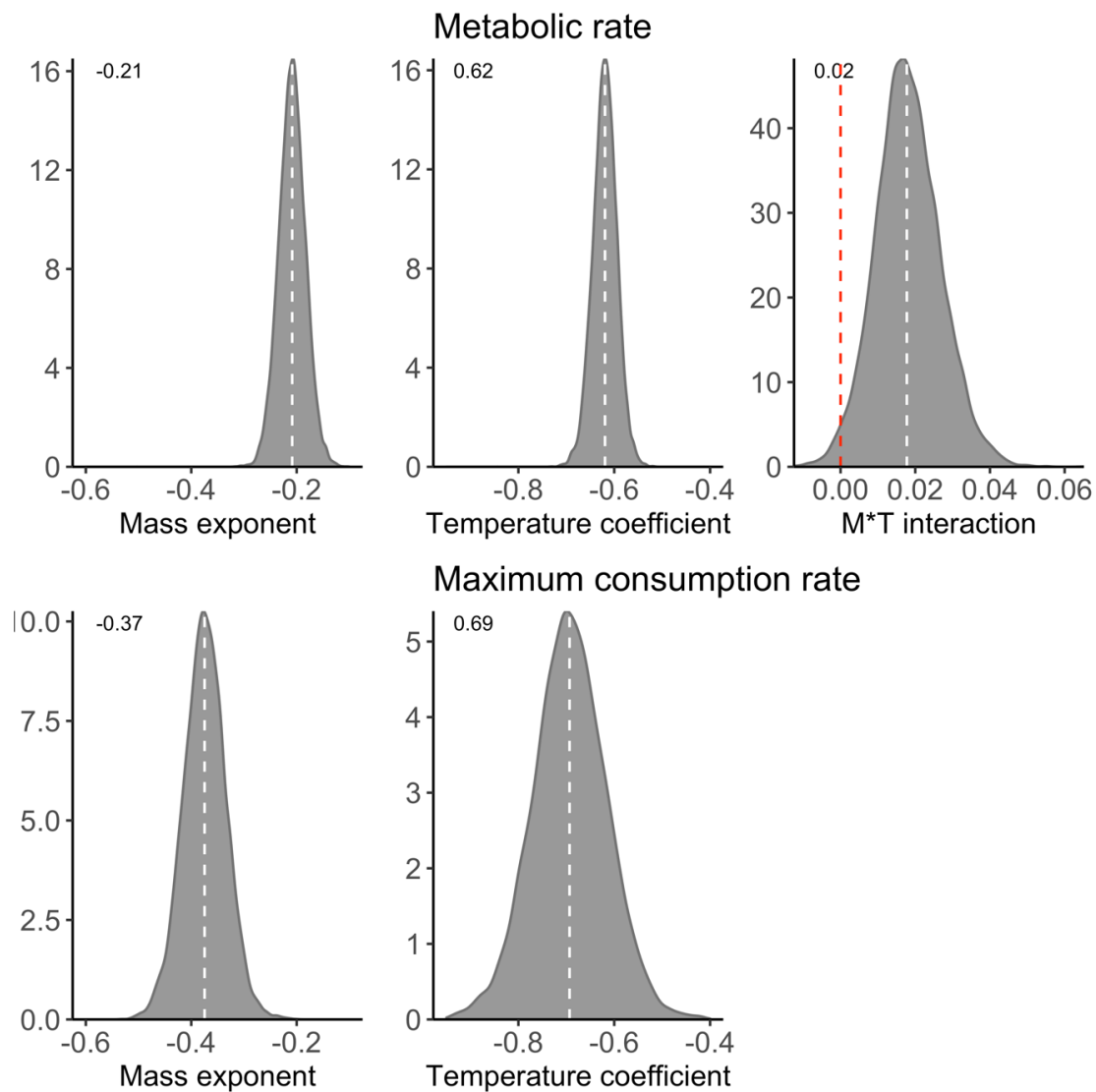


**Fig. S5.** Posterior distributions of the global intraspecific mass-specific mass exponents ( $\mu_{\beta_1}$ ) and temperature coefficients ( $\mu_{\beta_2}$ ) for metabolic rate (top) and maximum consumption rate (bottom). For metabolism, the global interaction coefficient ( $\mu_{\beta_3}$ ) is also shown (estimated and presented on an Arrhenius temperature scale), but for consumption this term was not included in the selected model. Numbers in the top left corner correspond to the posterior median. The axes are the same for each parameter for comparison between the two rates.

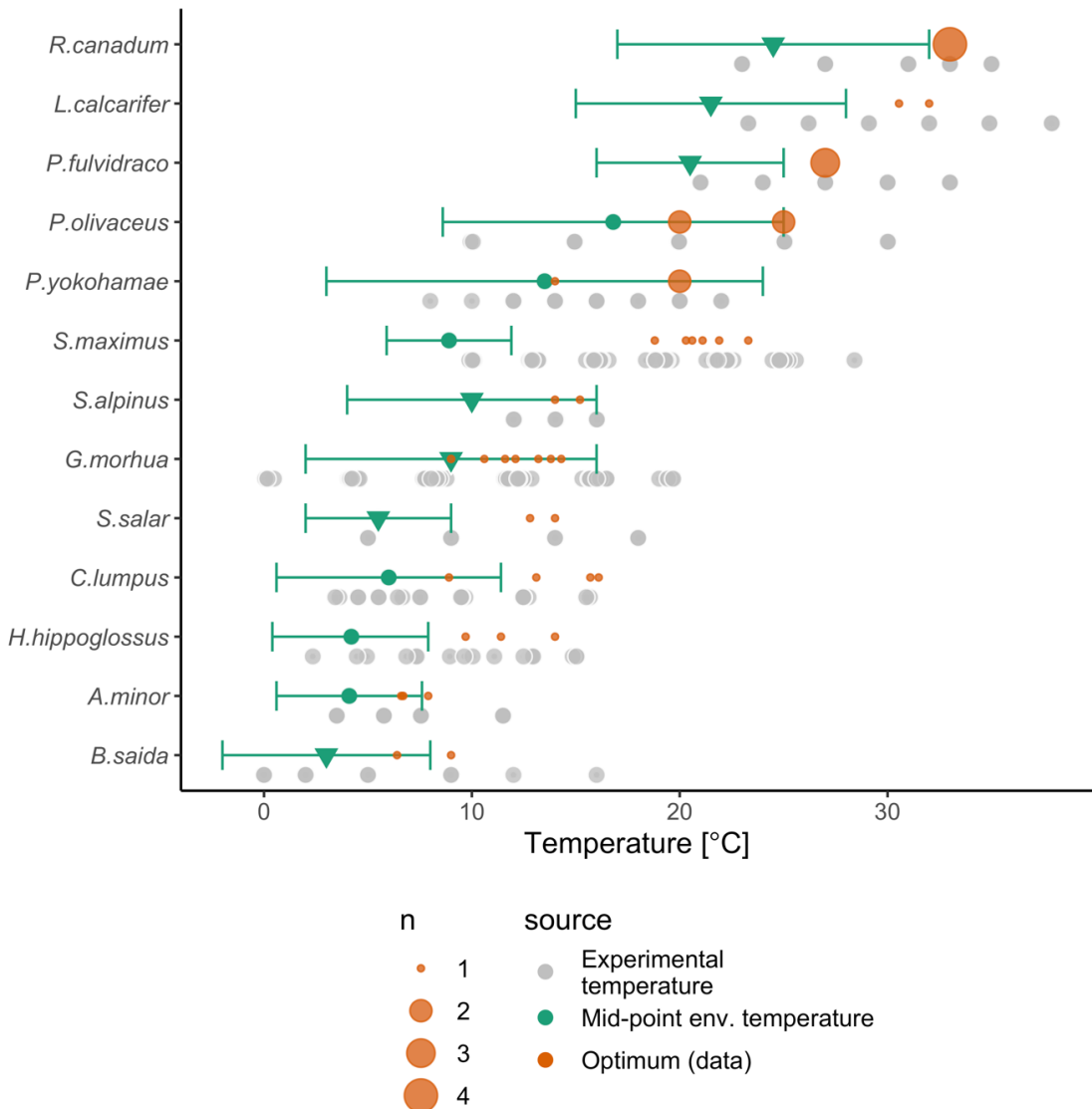


**Fig. S6.** Experimental temperatures (grey) overlap environmental temperatures (green), and optimum growth temperatures (orange) are typically at the upper end or above the environmental range. Horizontal green lines show the minimum and maximum environmental temperature based on either temperature in distribution range (triangles) or modelled distribution maps (circles), both taken from FishBase. The optimum growth temperatures are depicted for all size-classes per species, where the circle size is proportional to number of observations at that temperature.

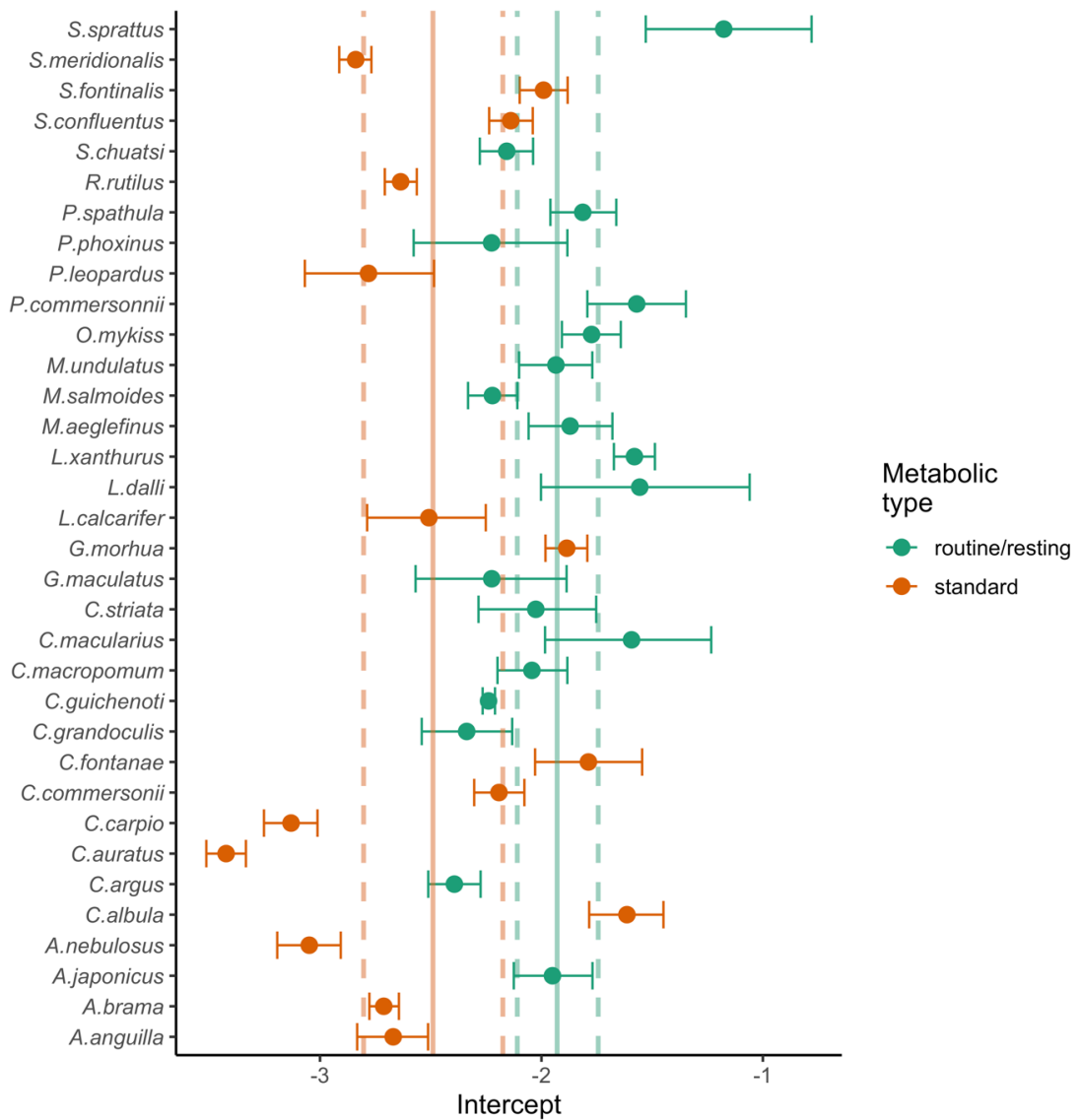


**Fig. S7.** Posterior median of species-level intercepts (points) and their 95% credible interval (horizontal error bars). Colors indicate the type of metabolism measurement for each species. Vertical solid lines are the posterior medians of the global intercepts (orange for standard metabolic rate,  $\mu_{\beta_{0s}}$ , and green for routine or resting metabolic rate,  $\mu_{\beta_{0r}}$ ), and the dashed vertical lines show the 95% credible intervals for the global parameters.

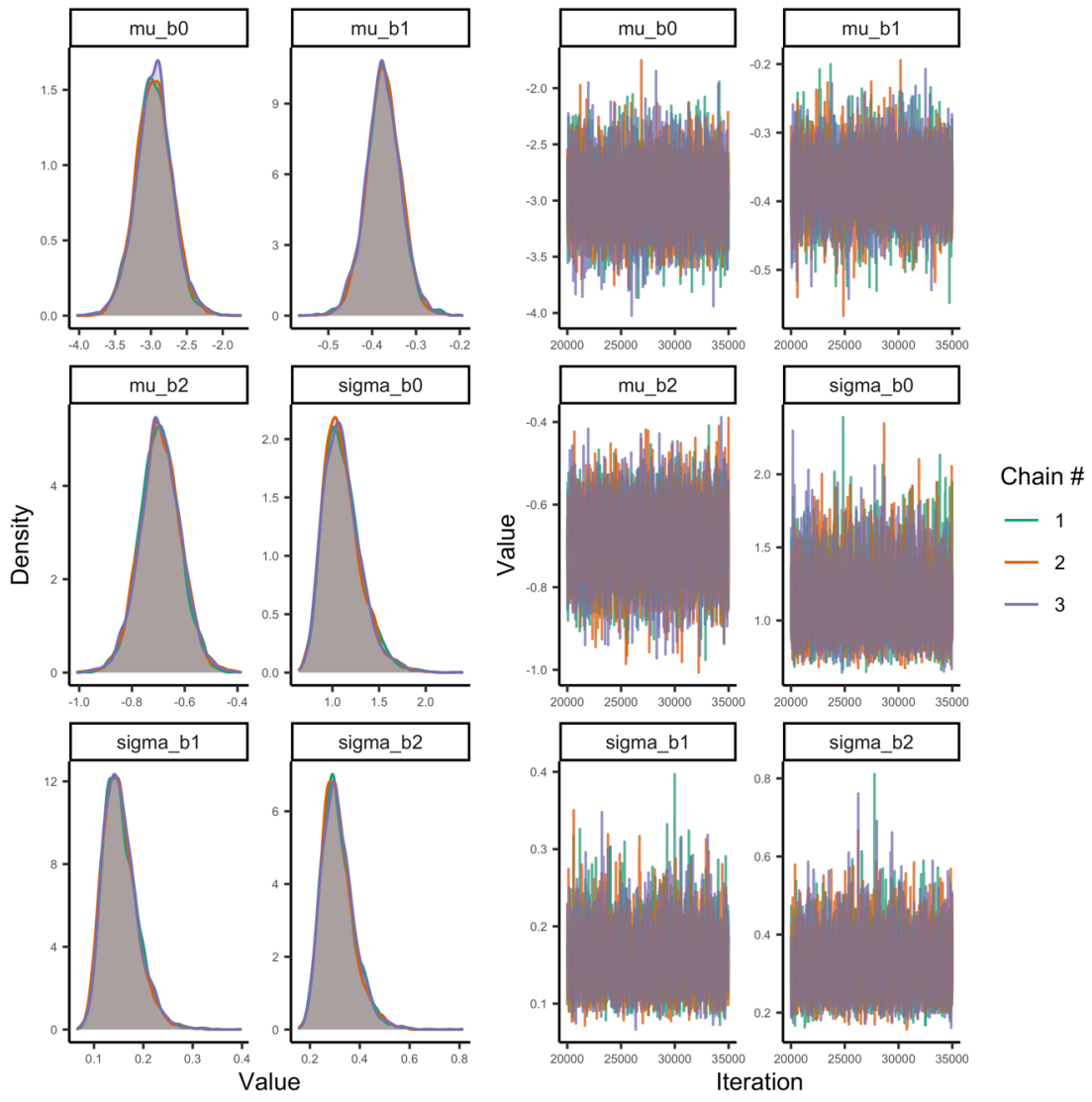


**Fig. S8.** Posterior densities and trace plots for evaluation of chain convergence (by chain, indicated by color), for the global-level parameters for the log-linear maximum consumption rate model at temperatures below peak temperatures.

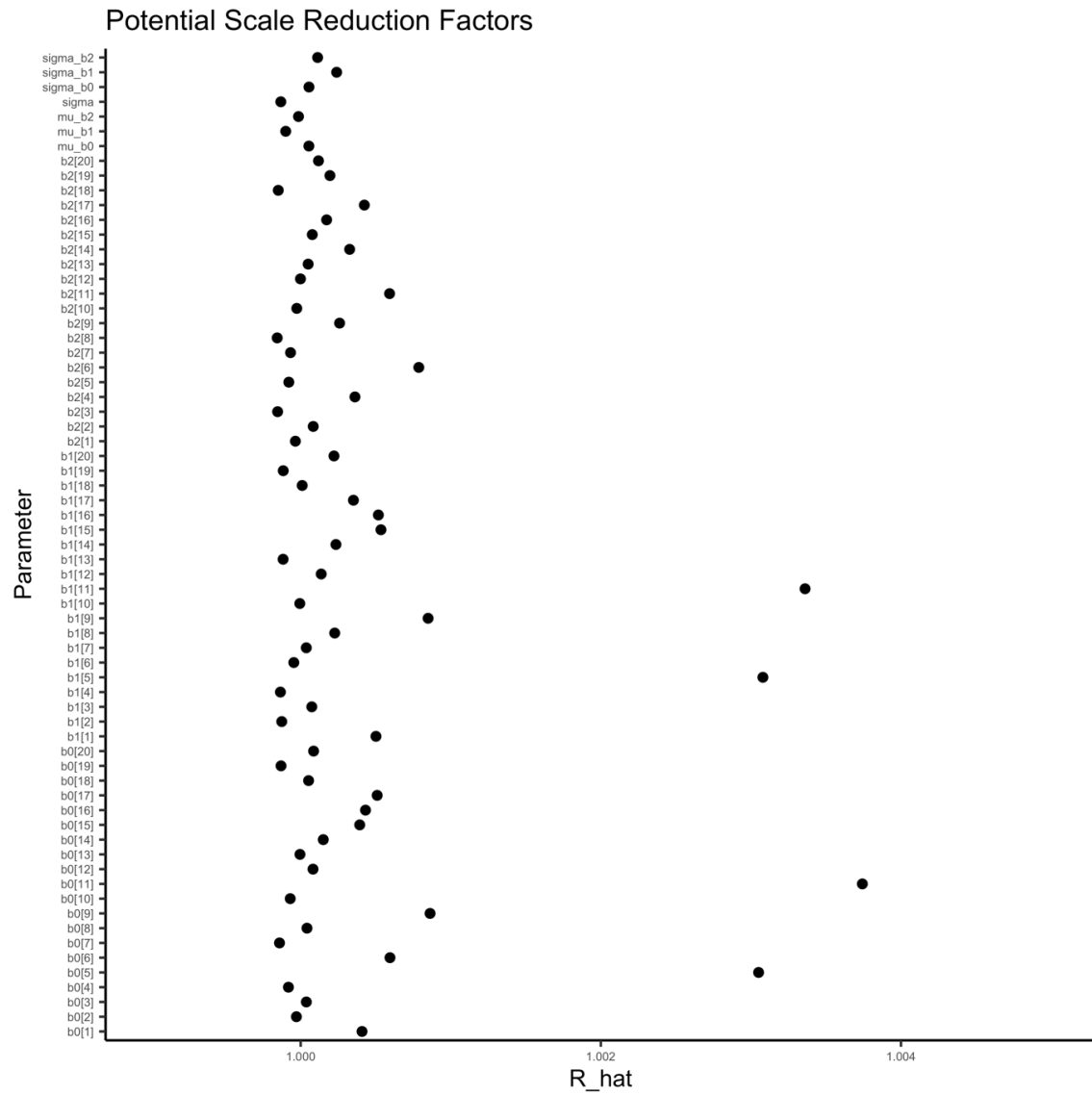


**Fig. S9.** Potential scale reduction factor ( $\hat{R}$ ) for the log-linear maximum consumption rate model. This factor is based on the comparison of between and within-chain variation for the same parameter. A value close to one implies chains converged to the same distribution. The index of the parameter corresponds to species. The index of the parameter corresponds to species in alphabetical order.

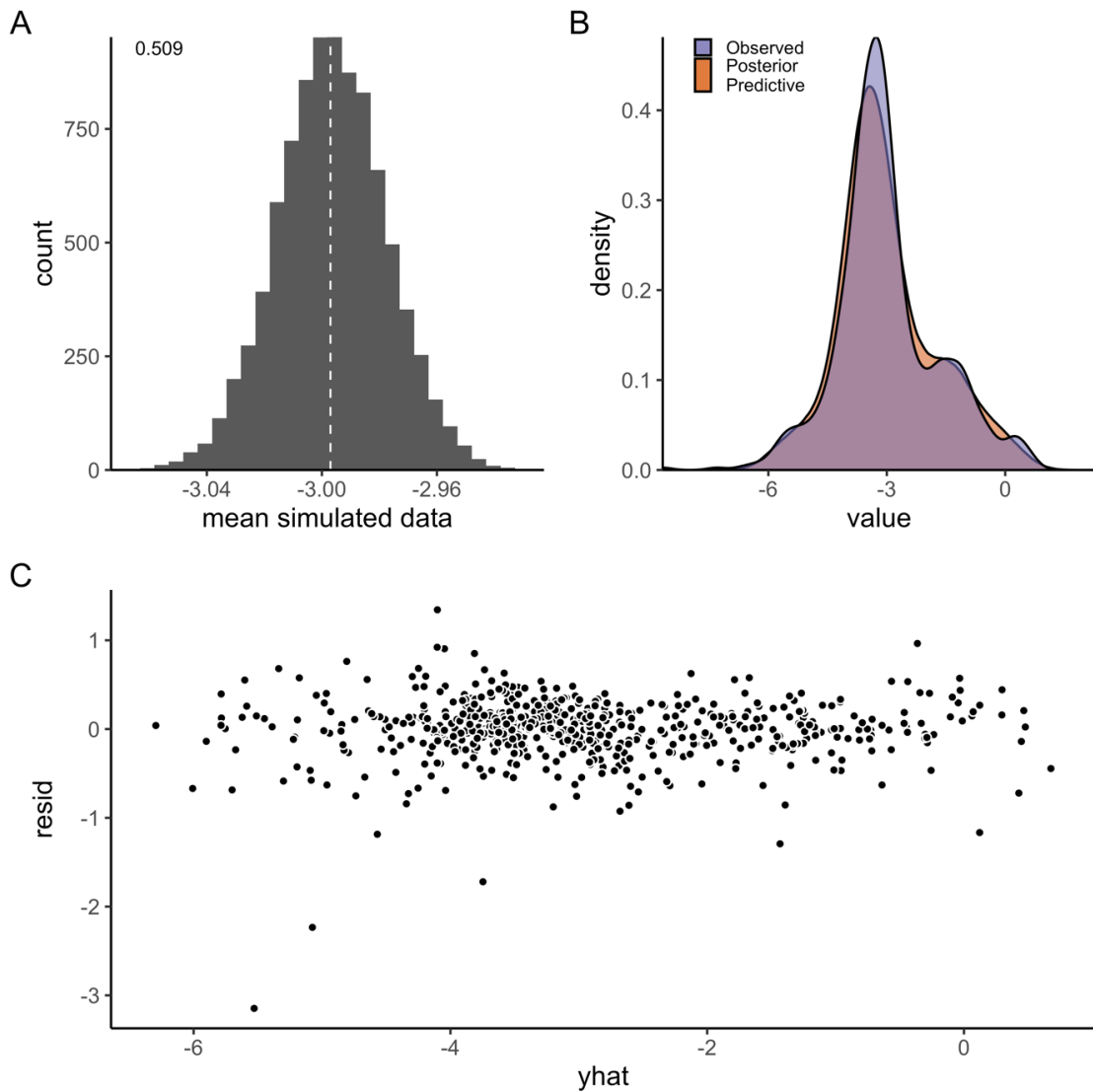


**Fig. S10.** A) Model fit (mean) for the log-linear model of maximum consumption rate at temperatures below temperature peak (by species). Fit is evaluated by simulating data from the likelihood (at each iteration of the MCMC chain), to compare how well it matches the original data. Each simulated data point is assigned a 0 or 1 if it is below or above the mean data point (the vertical line corresponds to the mean in data). The number in the plot corresponds to the mean of the vector of 0's and 1's. B) Posterior predictive distribution (orange) and distribution of data (purple). C) Difference between the observed value and the posterior median of the predicted value, plotted against fitted value.

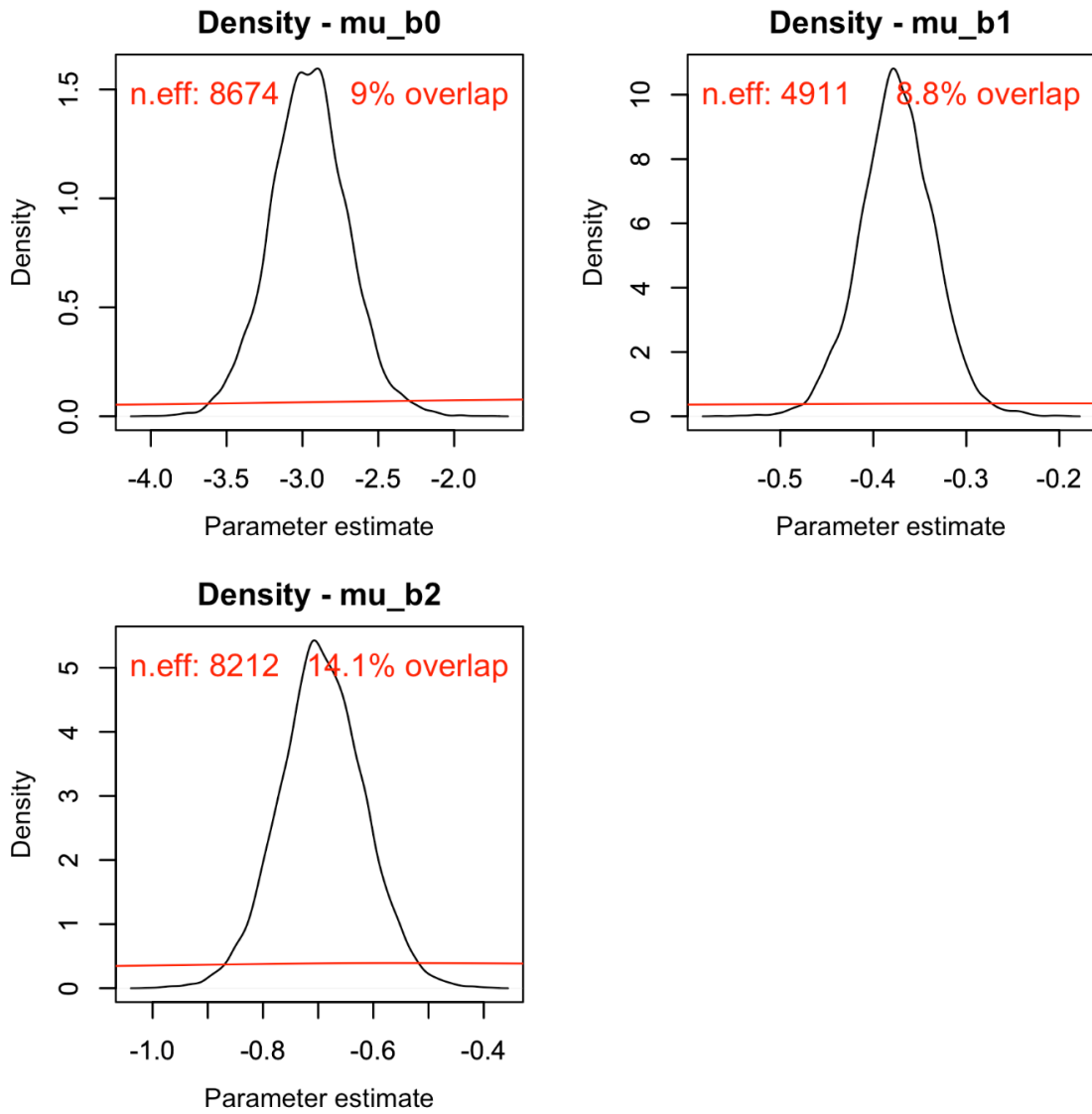


**Fig. S11.** Posterior (black) and prior distribution (red) for the global parameters in the log-linear model for maximum consumption rate, including their % overlap and effective sample size (n.eff).

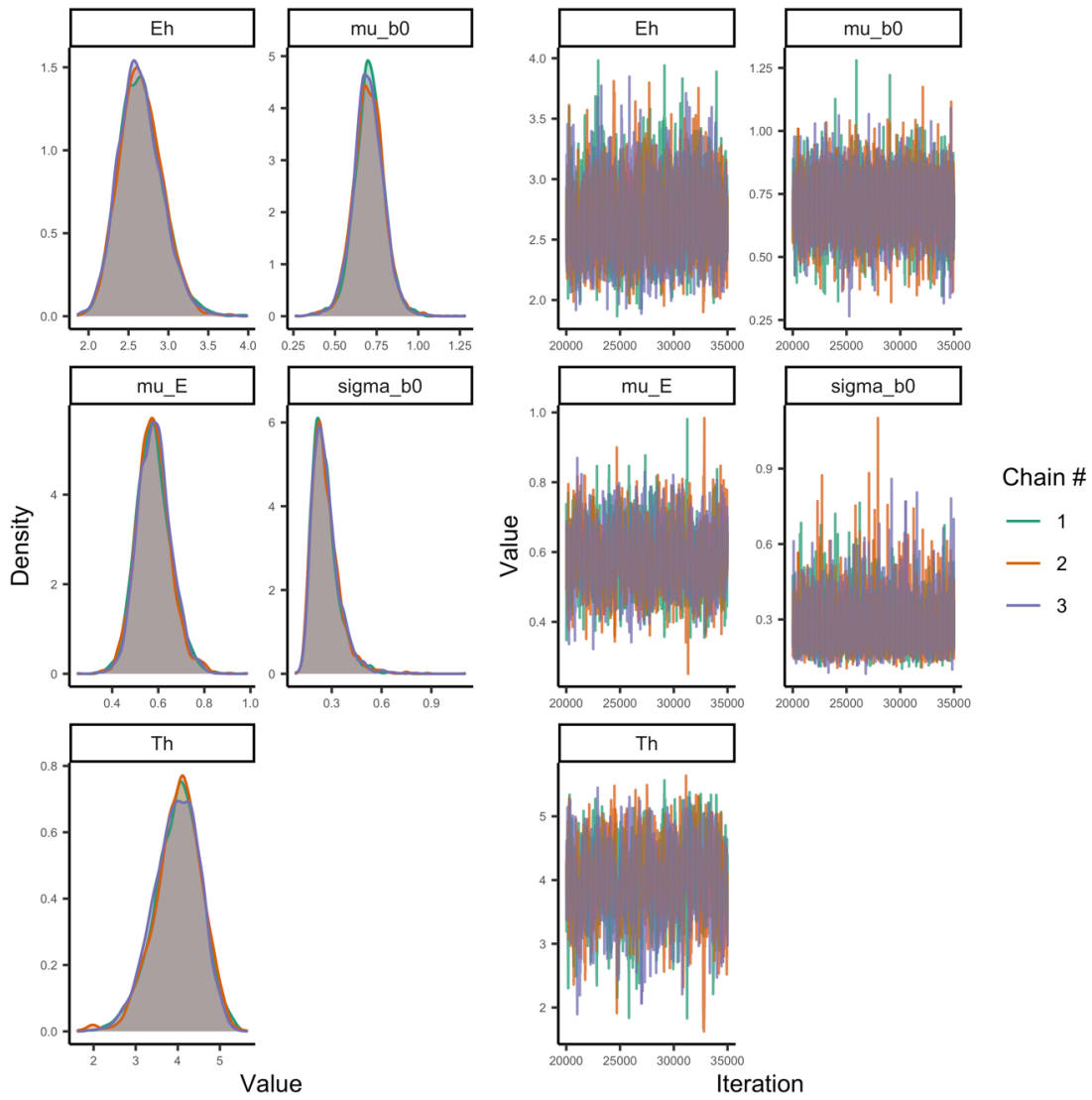


**Fig. S12.** Posterior densities and trace plots for evaluation of chain convergence (by chain, indicated by color), for the global-level parameters for the Sharpe-Schoolfield model fitted to maximum consumption rate data with temperatures including beyond peak temperatures.

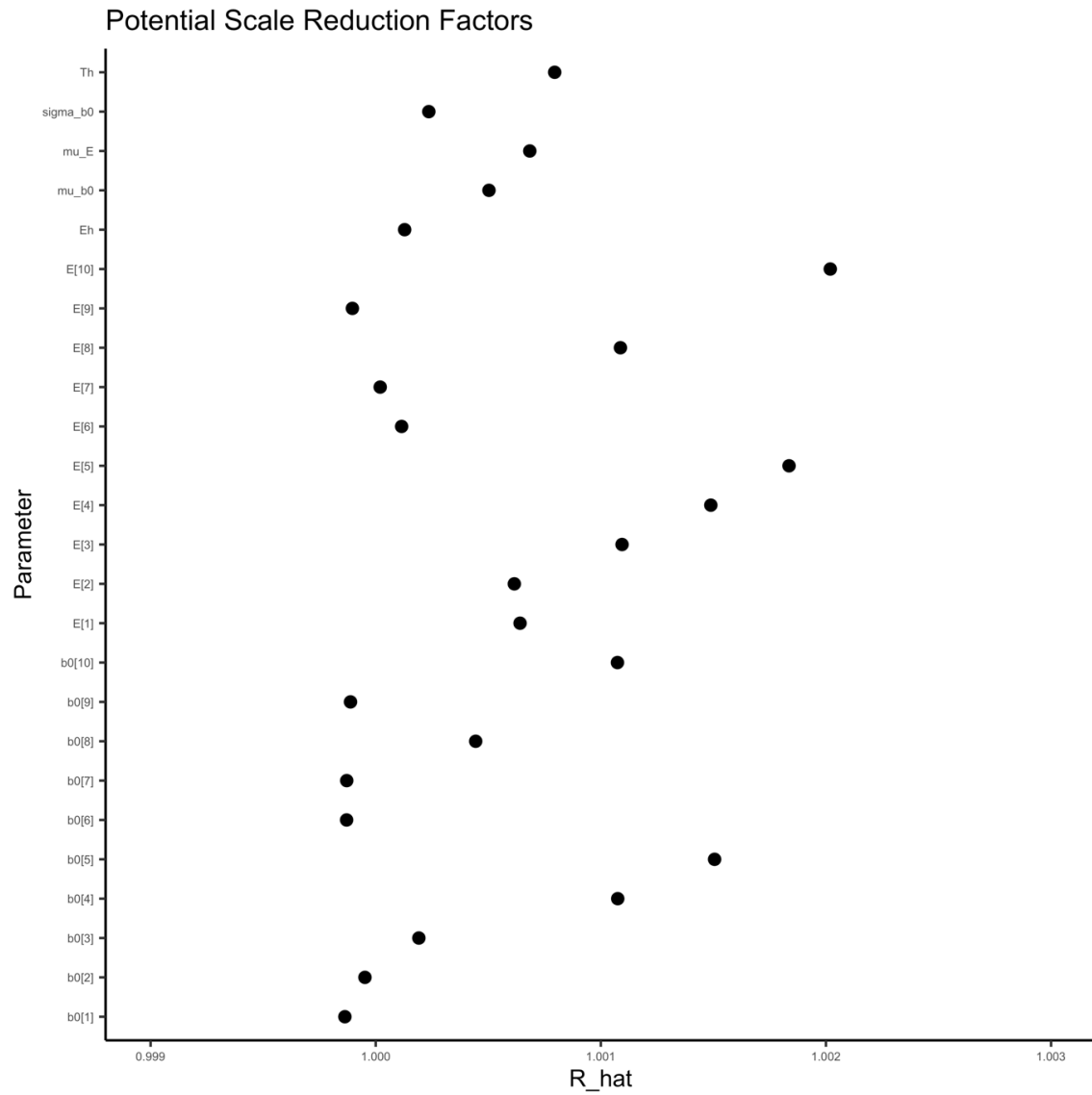


**Fig. S13.** Potential scale reduction factor ( $\hat{R}$ ) for the Sharpe-Schoolfield model fitted to maximum consumption rate data (including data beyond peak). This factor is based on the comparison of between and within-chain variation for the same parameter. A value close to one implies chains converged to the same distribution. The index of the parameter corresponds to species in alphabetical order.

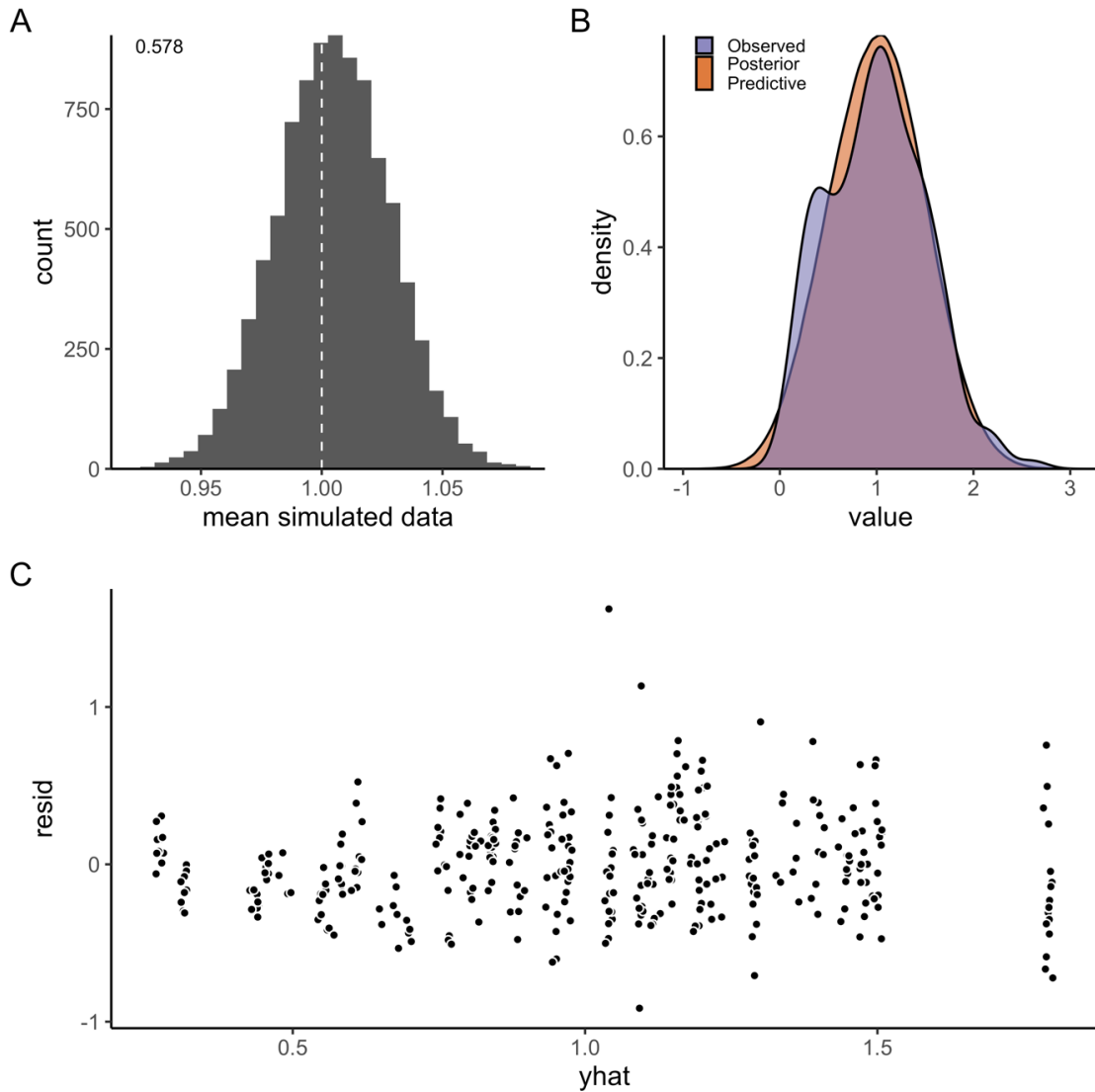


**Fig. S14.** A) Model fit (mean) for the Sharpe-Schoolfield model fitted to maximum consumption rate data including temperatures beyond peak (by species). Fit is evaluated by simulating data from the likelihood (at each iteration of the MCMC chain), to compare how well it matches the original data. Each simulated data point is assigned a 0 or 1 if it is below or above the mean data point (the vertical line corresponds to the mean in data). The number in the plot corresponds to the mean of the vector of 0's and 1's. B) Posterior predictive distribution (orange) and distribution of data (purple). C) Difference between the observed value and the posterior median of the predicted value, plotted against fitted value.

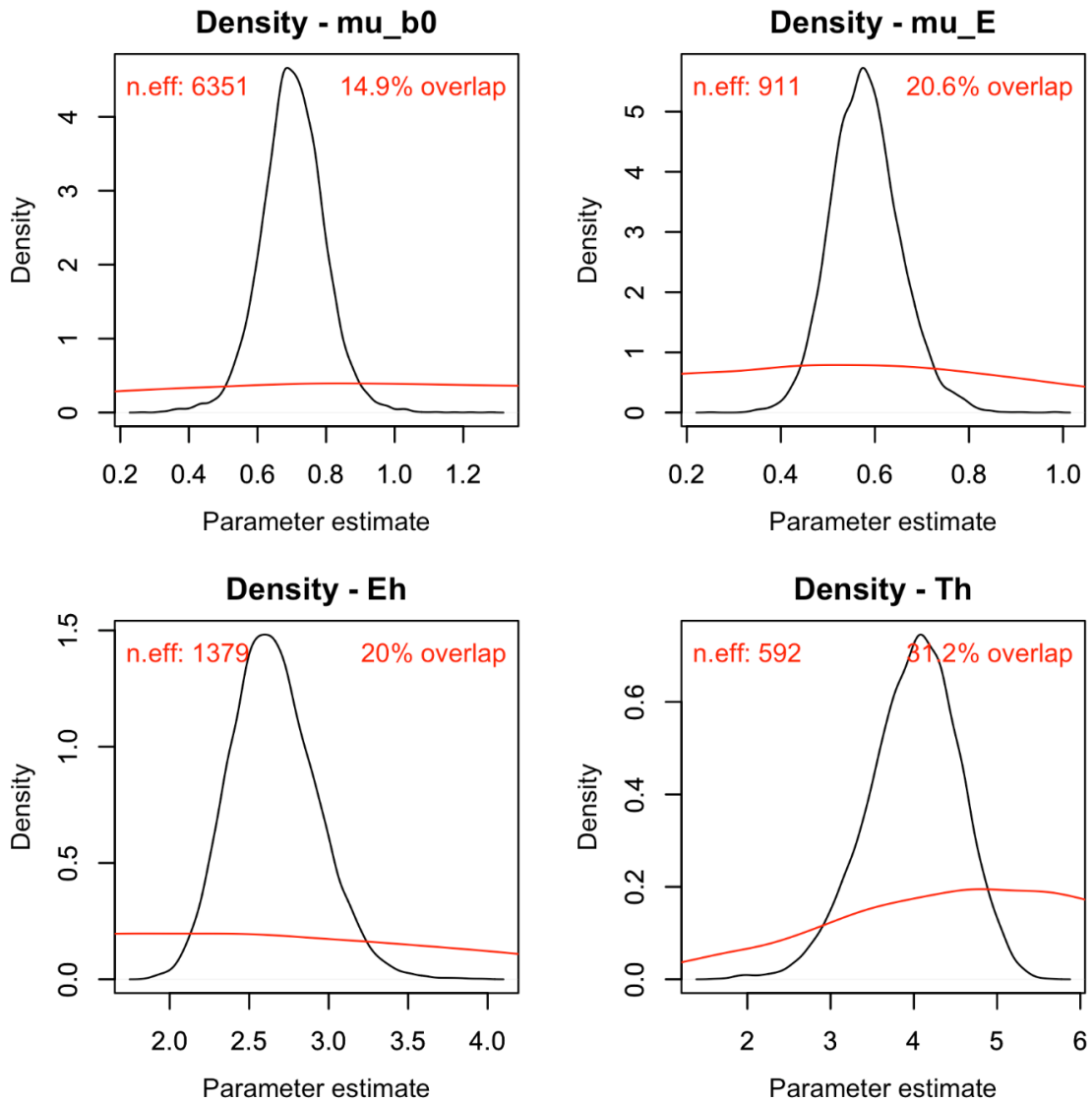


**Fig. S15.** Posterior (black) and prior distribution (red) for the global parameters in the Sharpe-Schoolfield model for maximum consumption rate including data beyond peak, including their % overlap (rounded) and effective sample size (n.eff).

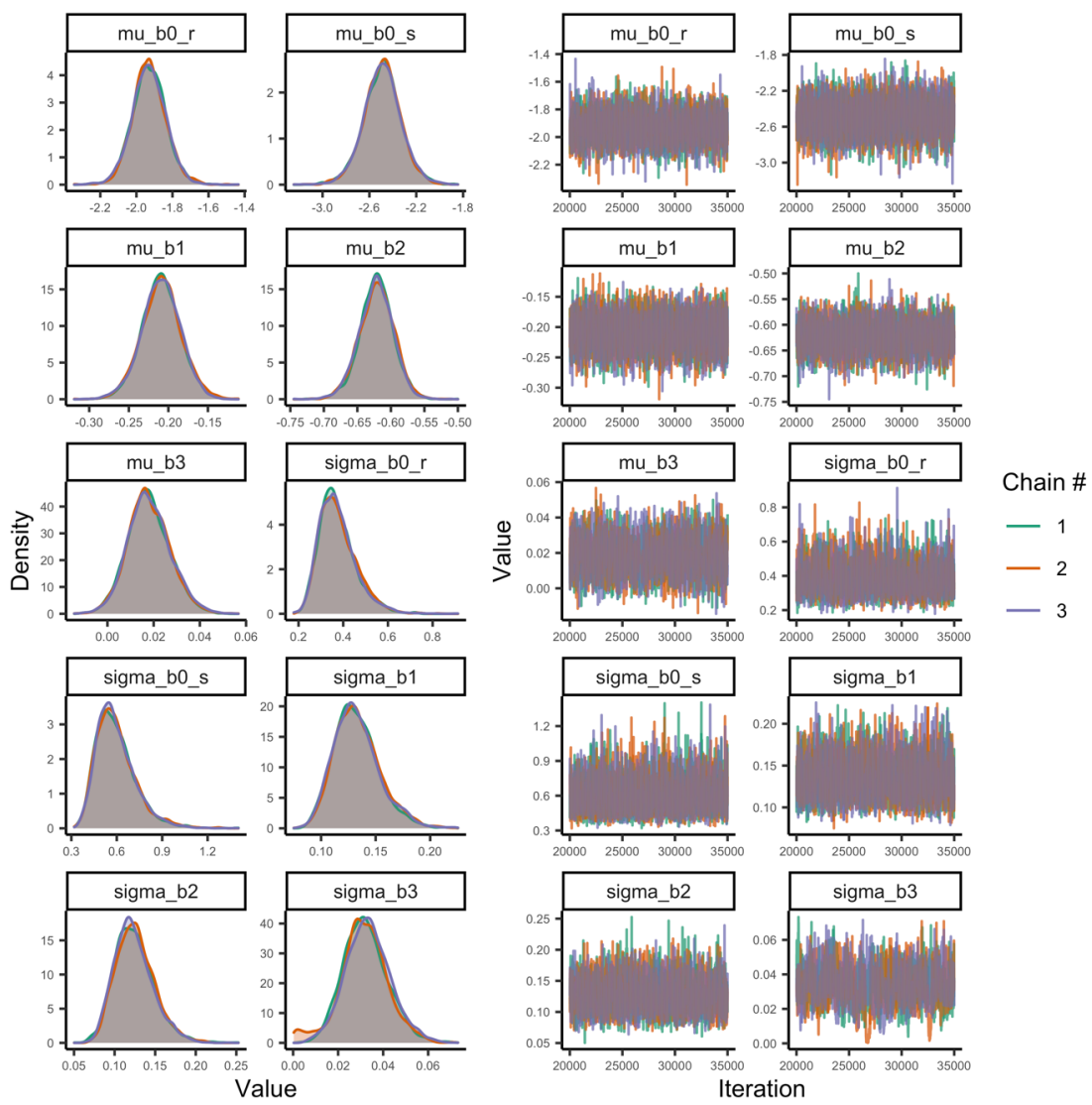


**Fig. S16.** Posterior densities and trace plots for evaluation of chain convergence (by chain, indicated by color), for the global-level parameters for the metabolic rate model at temperatures below peak temperatures.

### Potential Scale Reduction Factors

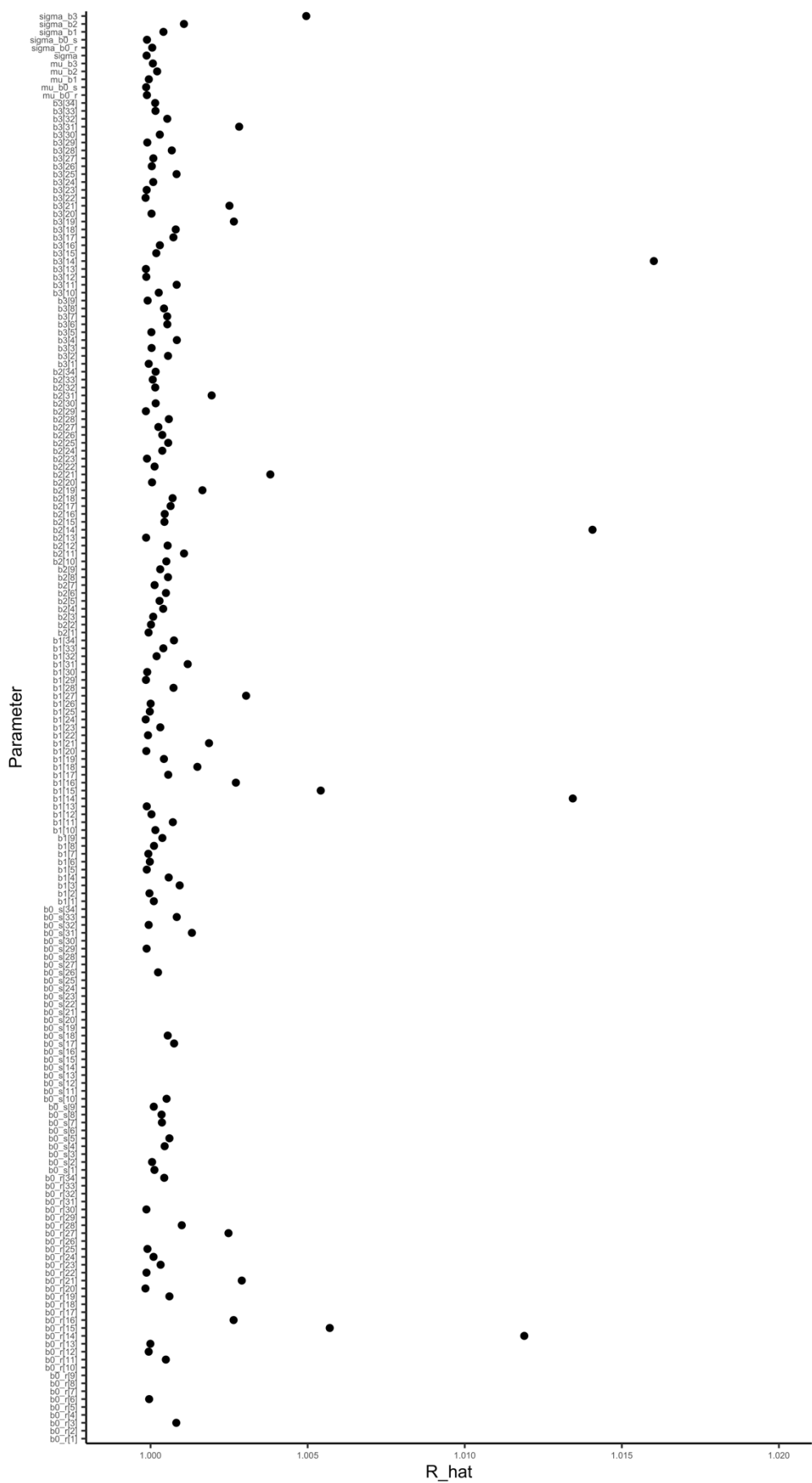


**Fig. S17.** Potential scale reduction factor ( $\hat{R}$ ) for the metabolic rate model. This factor is based on the comparison of between and within-chain variation for the same parameter. A value close to one implies chains converged to the same distribution. The index of the parameter corresponds to species in alphabetical order.

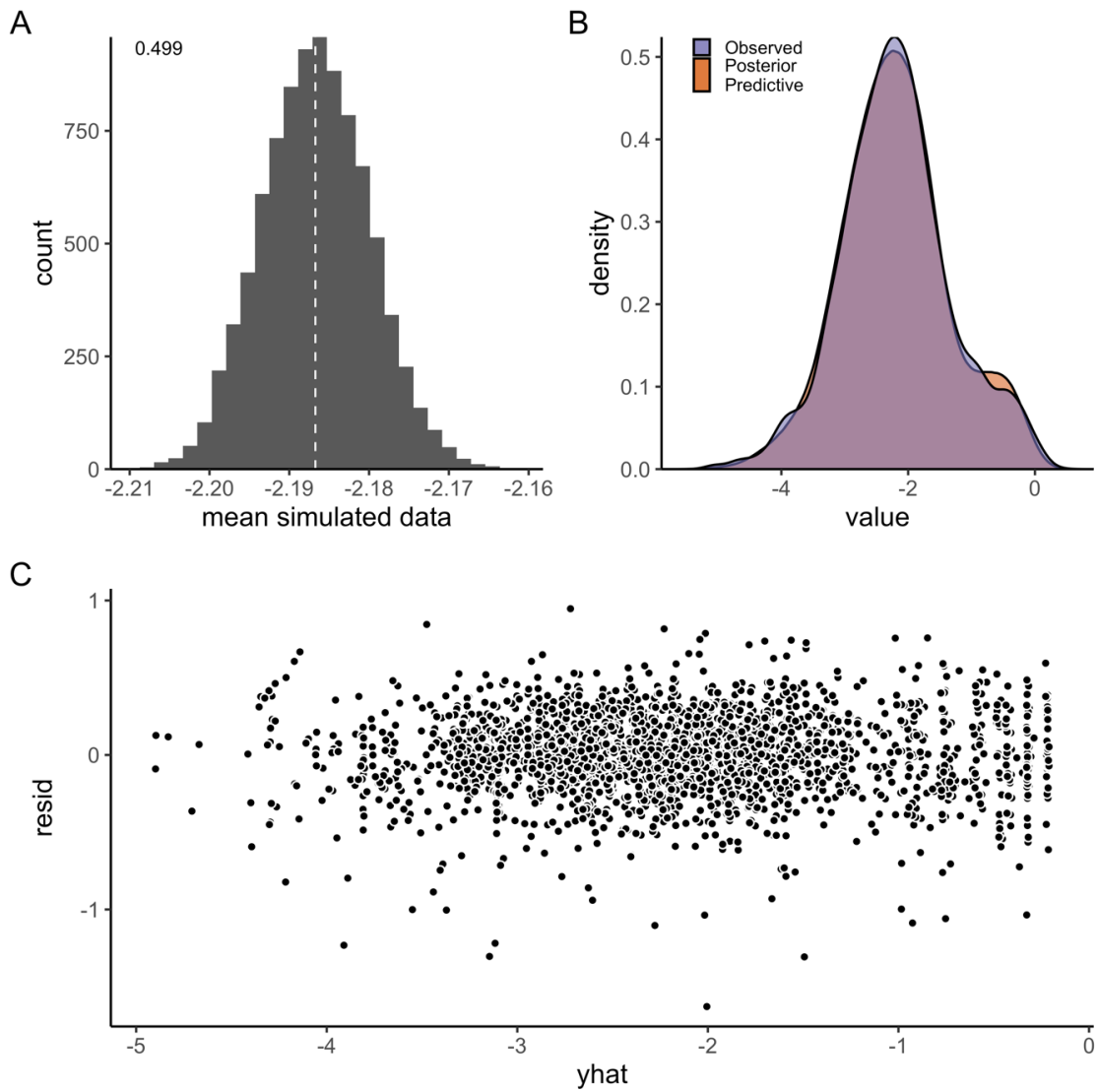


**Fig. S18.** A) Model fit (mean) for the log-linear model of metabolic rate. Fit is evaluated by simulating data from the likelihood (at each iteration of the MCMC chain), to compare how well it matches the original data. Each simulated data point is assigned a 0 or 1 if it is below or above the mean data point (the vertical line corresponds to the mean in data). The number in the plot corresponds to the mean of the vector of 0's and 1's. B) Posterior predictive distribution (orange) and distribution of data (purple). C) Difference between the observed value and the posterior median of the predicted value, plotted against fitted value.

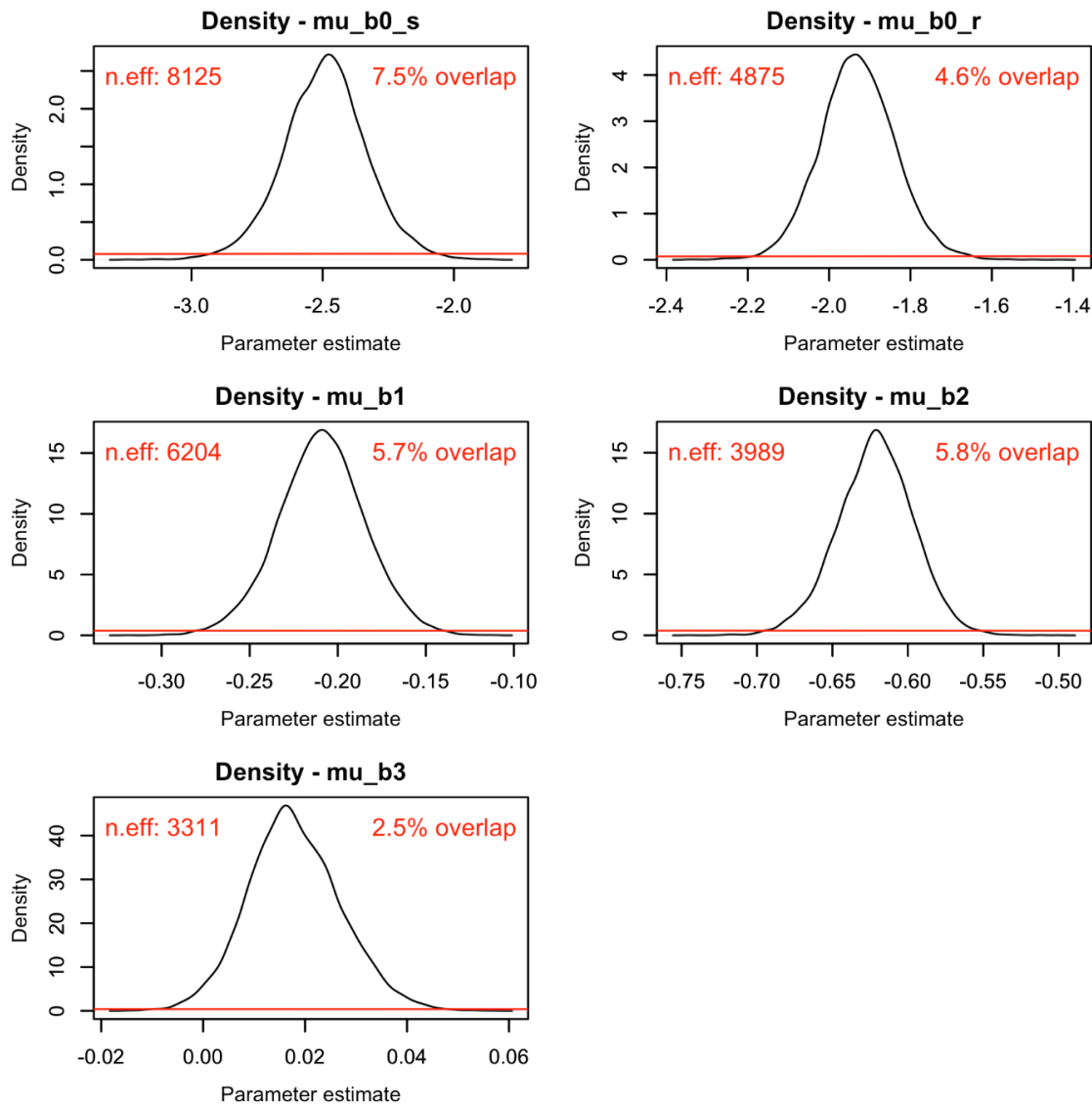


**Fig. S19.** Posterior (black) and prior distribution (red) for the global parameters in the model for metabolic rate, including their % overlap and effective sample size (n.eff).

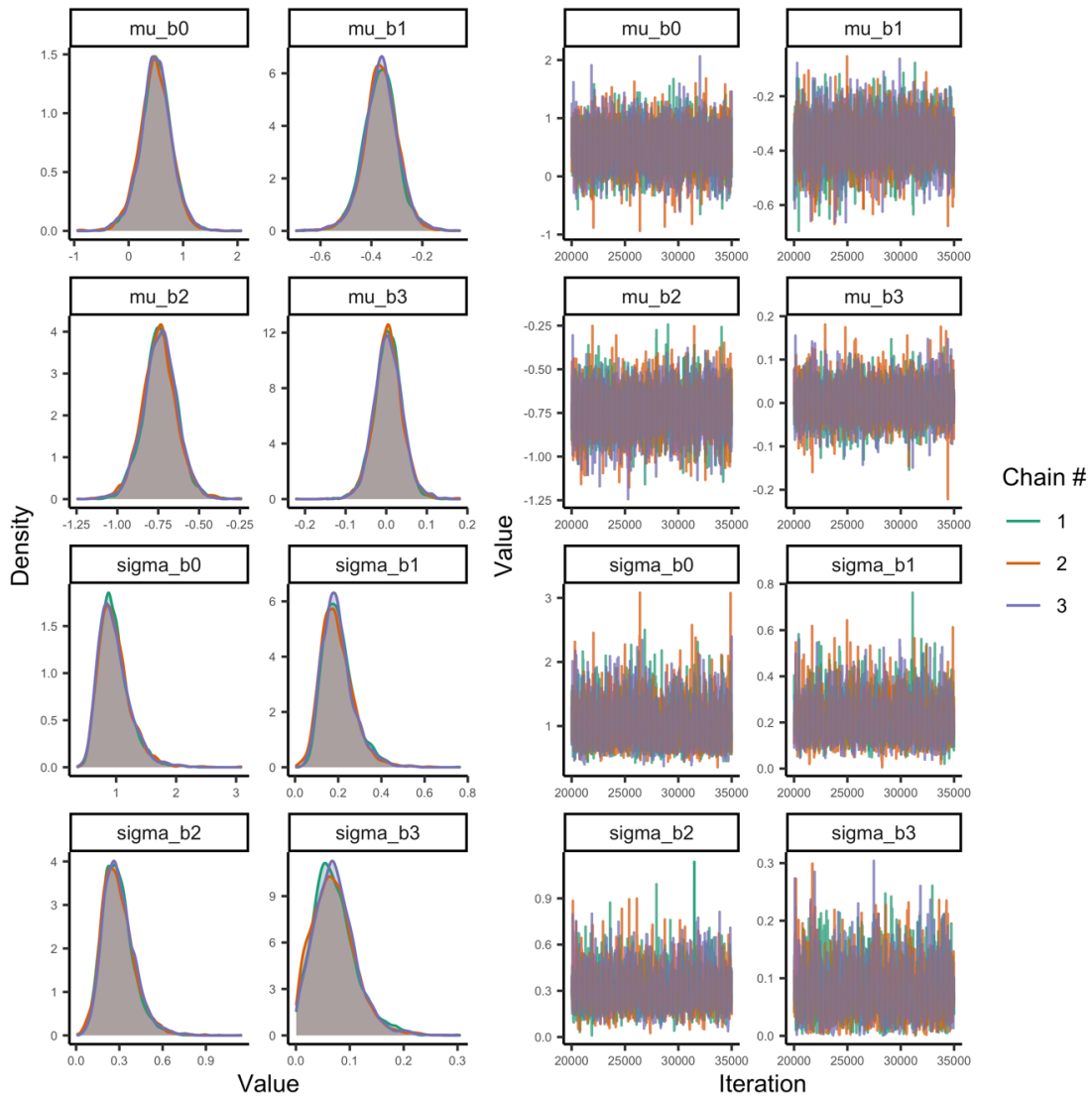


**Fig. S20.** Posterior densities and trace plots for evaluation of chain convergence (by chain, indicated by color), for the global-level parameters for the growth rate model at temperatures below optimum temperatures.

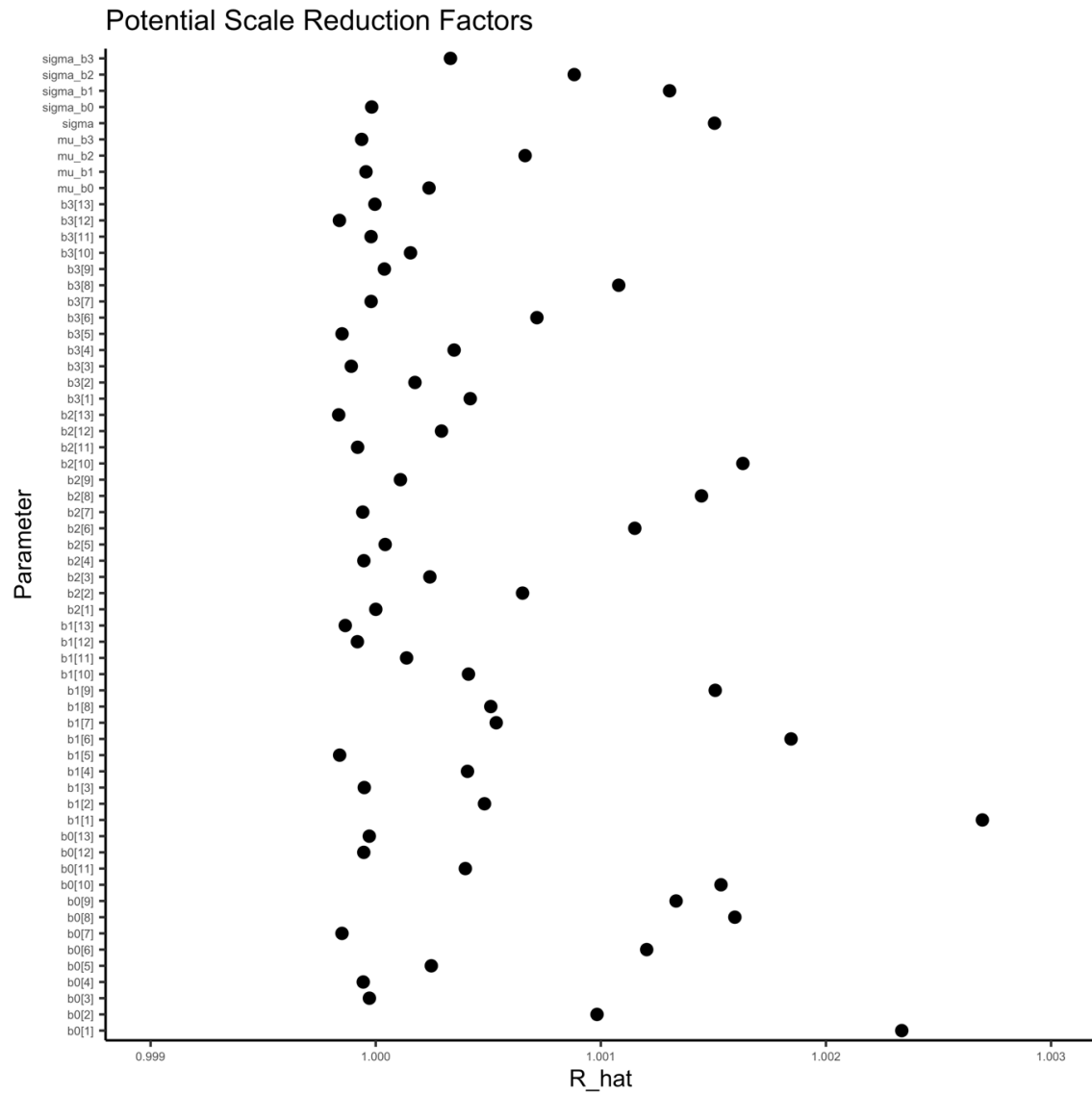


**Fig. S21.** Potential scale reduction factor ( $\hat{R}$ ) for the growth rate model. This factor is based on the comparison of between and within-chain variation for the same parameter. A value close to one implies chains converged to the same distribution. The index of the parameter corresponds to species in alphabetical order.

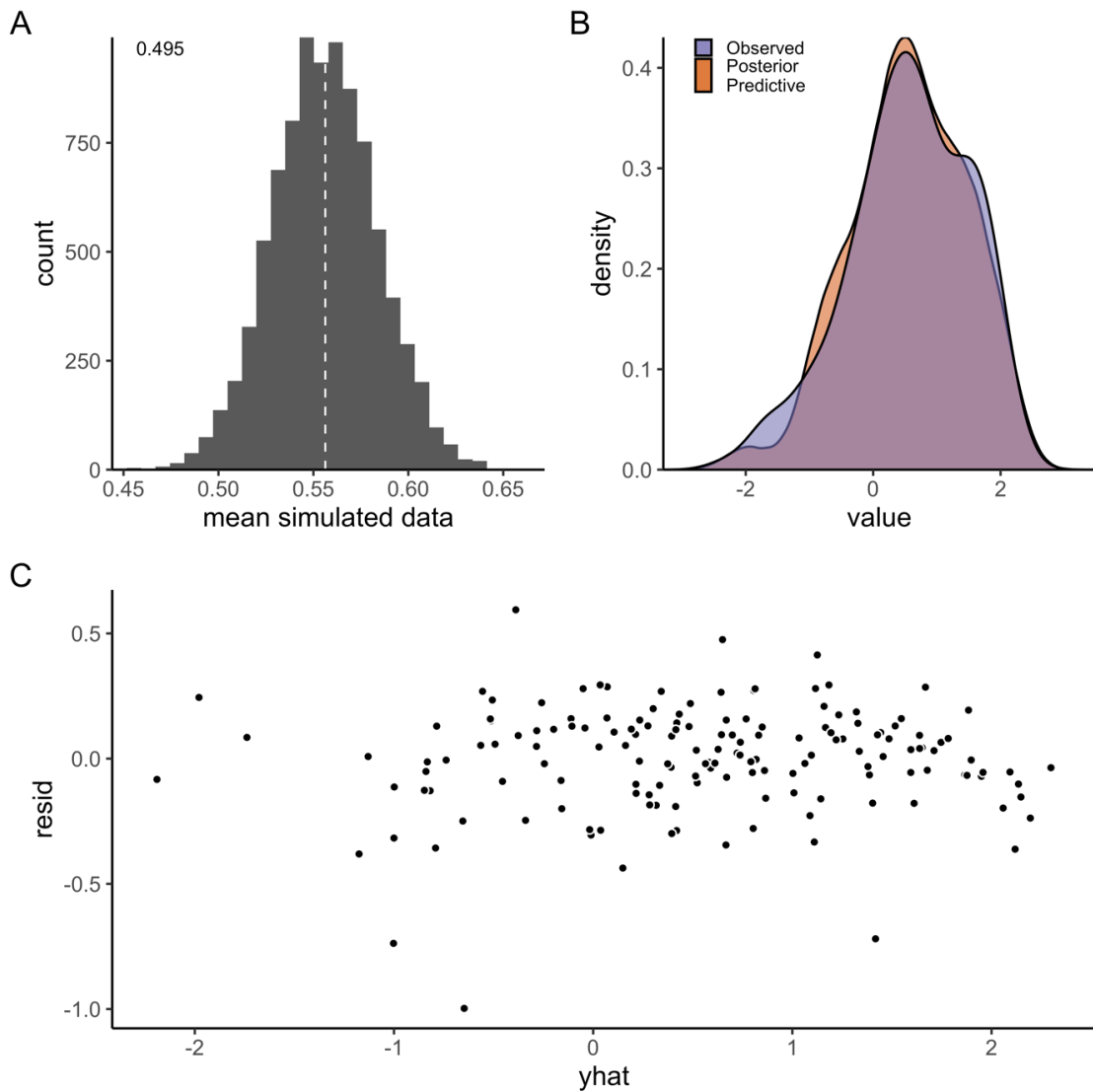


**Fig. S22.** A) Model fit (mean) for the model of growth at temperatures below temperature optimum (by species). Fit is evaluated by simulating data from the likelihood (at each iteration of the MCMC chain), to compare how well it matches the original data. Each simulated data point is assigned a 0 or 1 if it is below or above the mean data point (the vertical line corresponds to the mean in data). The number in the plot corresponds to the mean of the vector of 0's and 1's. B) Posterior predictive distribution (orange) and distribution of data (purple). C) Difference between the observed value and the posterior median of the predicted value, plotted against fitted value.

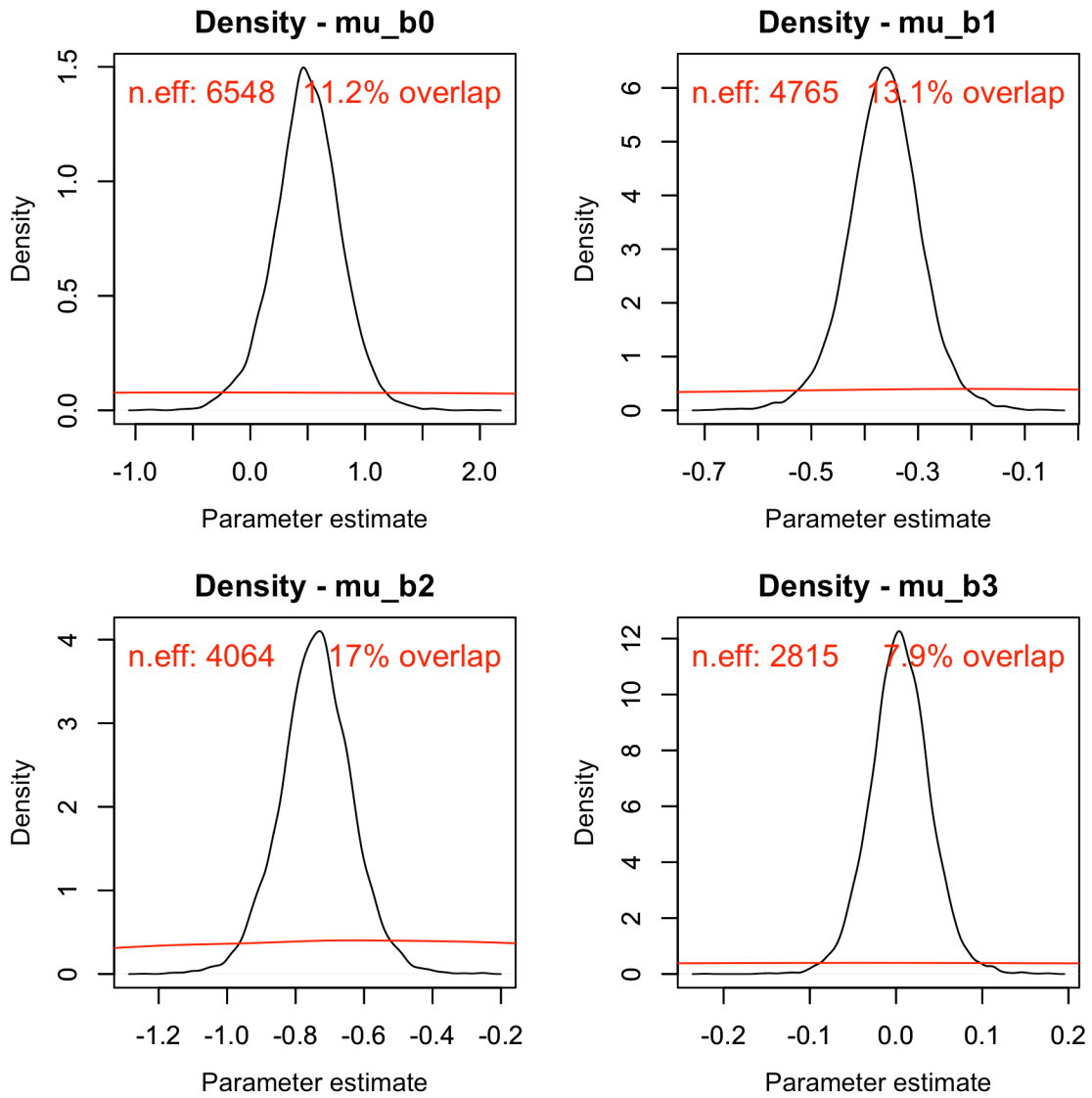


**Fig. S23.** Posterior (black) and prior distribution (red) for the global parameters in the model for growth rate, including their % overlap and effective sample size (n.eff).

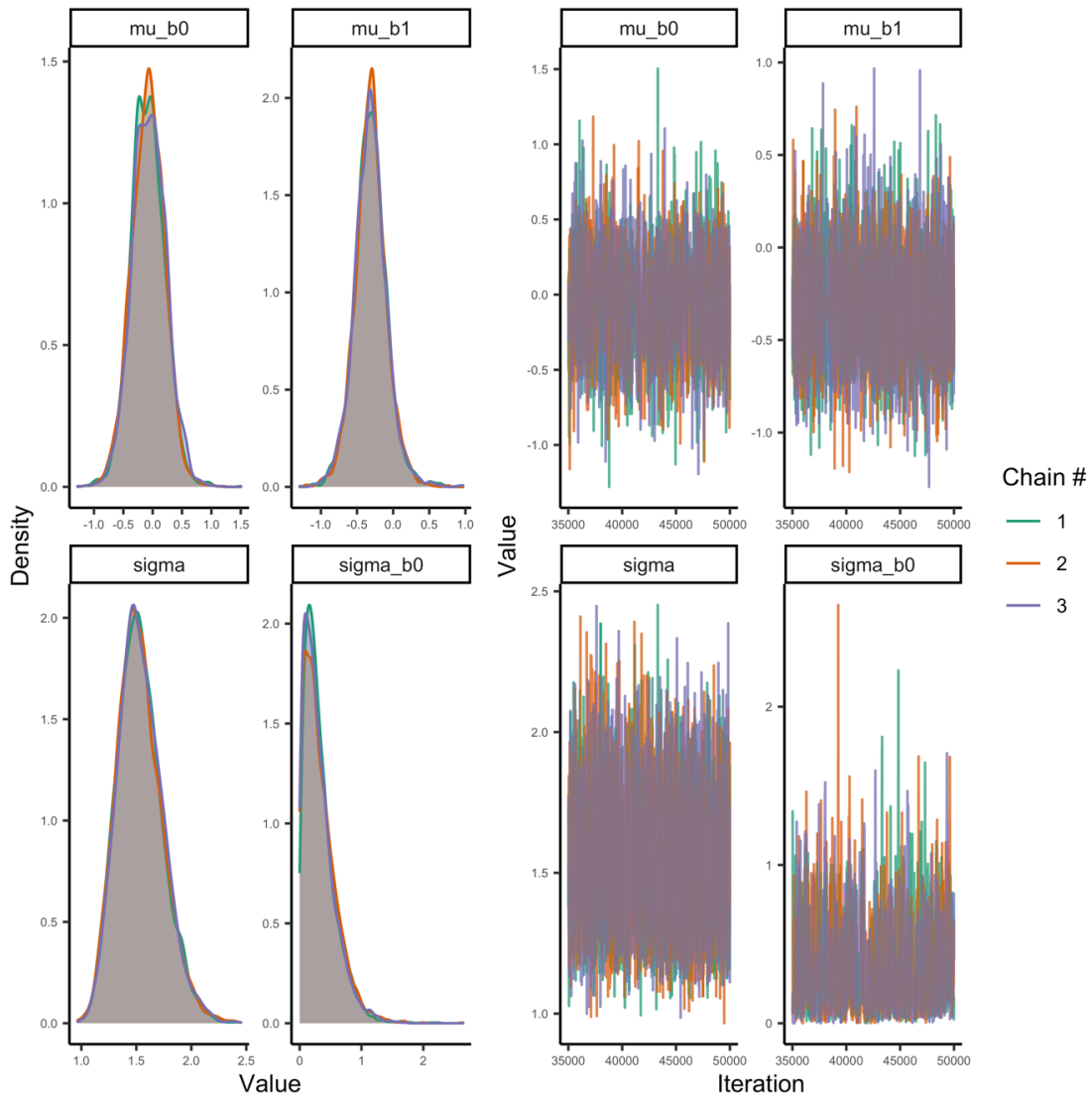


**Fig. S24.** Posterior densities and trace plots for evaluation of chain convergence (by chain, indicated by color), for the global-level parameters for the  $T_{opt}$  model.

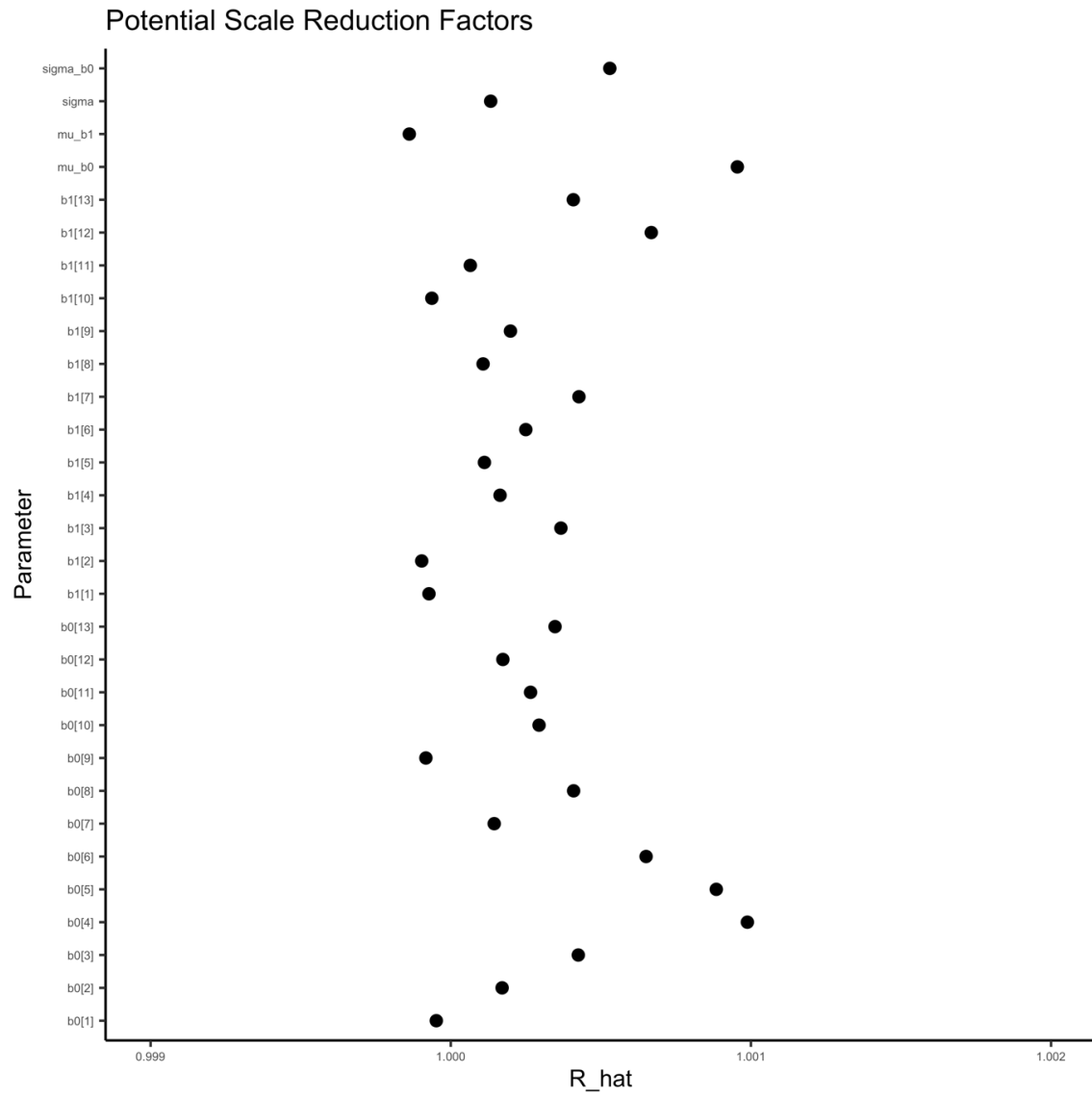


**Fig. S25.** Potential scale reduction factor ( $\hat{R}$ ) for the  $T_{opt}$  model. This factor is based on the comparison of between and within-chain variation for the same parameter. A value close to one implies chains converged to the same distribution. The index of the parameter corresponds to species in alphabetical order.

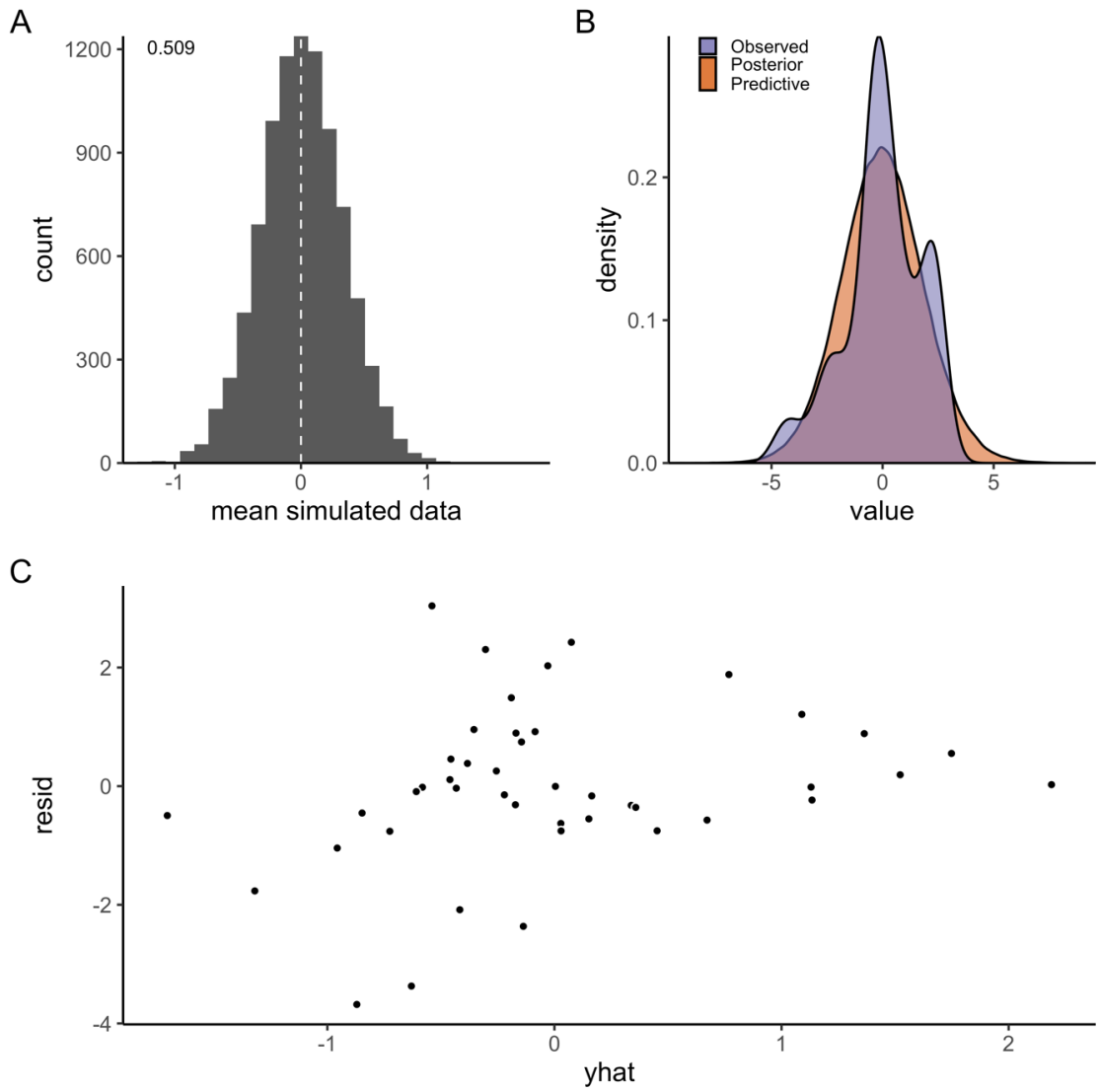


**Fig. S26.** A) Model fit (mean) for the model of optimum growth temperature as a function of body mass. Fit is evaluated by simulating data from the likelihood (at each iteration of the MCMC chain), to compare how well it matches the original data. Each simulated data point is assigned a 0 or 1 if it is below or above the mean data point (the vertical line corresponds to the mean in data). The number in the plot corresponds to the mean of the vector of 0's and 1's. B) Posterior predictive distribution (orange) and distribution of data (purple). C) Difference between the observed value and the posterior median of the predicted value, plotted against fitted value.

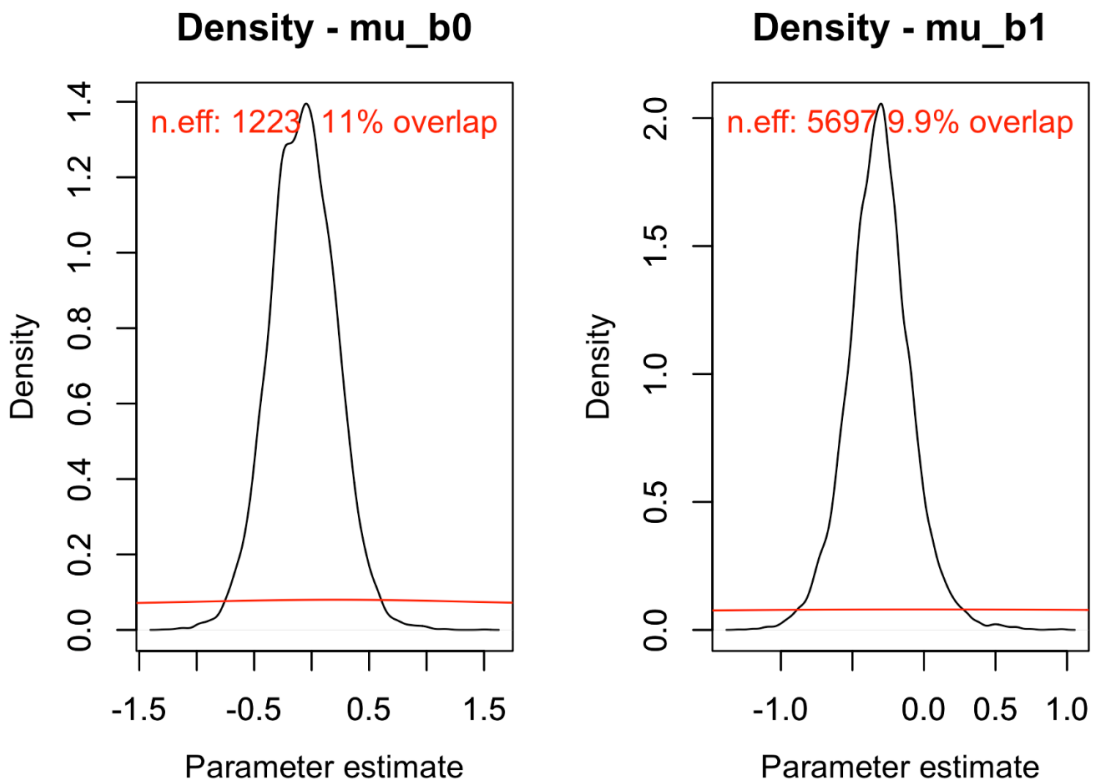


**Fig. S27.** Posterior (black) and prior distribution (red) for the global parameters in the model for  $T_{opt}$ , including their % overlap and effective sample size (n.eff).

**Table S1.** Explanation of data columns (G=growth data, T<sub>opt</sub>=optimum growth temperature data, C=maximum consumption data, M=metabolism data).

Column	Explanation	Datasets
<i>growth_rate %/day</i>	Main response variable.	G, T <sub>opt</sub>
<i>opt_temp_c</i>	Main response variable.	T <sub>opt</sub>
<i>initial_mass_g</i>	Body mass [g] at the onset of the growth trial.	G, T <sub>opt</sub>
<i>final_mass_g</i>	Body mass [g] at the end of the growth trial.	G, T <sub>opt</sub>
<i>geom_mean_mass_g</i>	Geometric mean mass in t <sub>1</sub> and t <sub>2</sub> of the growth trial.	G, T <sub>opt</sub>
<i>size_group</i>	Representative body mass of size group in the growth trial, in case initial, final or geometric body mass could not be retrieved.	G, T <sub>opt</sub>
<i>consumption</i>	Main response variable.	C
<i>metabolic_rate</i>	Main response variable.	M
<i>type</i>	Type of respiration measurement (resting, routine, standard).	M
<i>unit</i>	Unit of response variable.	C, M
<i>original_unit</i>	Original unit of response variable. If different from “ <i>unit</i> ”, see “ <i>notes</i> ” column for information on conversion.	C, M
<i>mass_g</i>	Body mass in experiment [g]. Some studies report body masses before and some after the feeding trials. See “ <i>notes</i> ”.	C, M
<i>temp_c</i>	Experimental temperature [°C].	G, C, M
<i>above_peak_temp</i>	Is the experiment conducted at temperature above peak temperature for the given size group? Y/N.	G, C, M
<i>common_name</i>	Common name of species.	G, T <sub>opt</sub> , C, M
<i>species</i>	Scientific name of species.	G, T <sub>opt</sub> , C, M
<i>genus</i>	Genus of species.	G, T <sub>opt</sub> , C, M
<i>family</i>	Family of species.	G, T <sub>opt</sub> , C, M
<i>order</i>	Order of species.	G, T <sub>opt</sub> , C, M
<i>habitat</i>	Species natural habitat, taken from FishBase (4).	G, T <sub>opt</sub> , C, M
<i>lifestyle</i>	Lifestyle of species, taken from FishBase (4).	G, T <sub>opt</sub> , C, M
<i>biogeography</i>	Biogeography of species, taken from FishBase (4).	G, T <sub>opt</sub> , C, M
<i>trophic_level</i>	Trophic level of species, taken from FishBase (4).	G, T <sub>opt</sub> , C, M
<i>w_maturity_g</i>	Body mass [g] at maturation taken from FishBase (4). If not available, weight was estimated from length using species-specific allometric weight-length, else taken from alternative sources (see “ <i>notes</i> ”). Used to estimate relative body size across species in the data and to normalize optimum growth temperatures across species.	G, T <sub>opt</sub>

<b>w_max_published_g</b>	Max. published weight [g] taken from FishBase (4). If not available, weight was estimated from length using species-specific allometric weight-length, else taken from alternative sources (see " <b>notes</b> "). Used to estimate relative body size across species in the data.	G, T <sub>opt</sub> , C, M
<b>env_temp_min</b>	Min. environmental temperature [°C], taken from FishBase (4). If not available on FishBase, data were taken from alternative sources (see " <b>notes</b> "). Used to compare experimental temperatures to common temperatures for species.	G, T <sub>opt</sub> , C, M
<b>env_temp_max</b>	Max. environmental temperature [°C], taken from FishBase (4). If not available on FishBase, data were taken from alternative sources (see " <b>notes</b> "). Used to compare experimental temperatures to common temperatures for species.	G, T <sub>opt</sub> , C, M
<b>env_temp_mid</b>	Median of environmental temperature [°C], taken from FishBase (4). If not available on FishBase, data were taken from alternative sources (see " <b>notes</b> "). Used to compare experimental temperatures to common temperatures for species.	G, T <sub>opt</sub> , C, M
<b>pref_temp_mid</b>	Median of preferred temperature [°C], taken from FishBase (4). If not available on FishBase, data were taken from alternative sources (see " <b>notes</b> "). Used to compare experimental temperatures to common temperatures for species.	G, T <sub>opt</sub> , C, M
<b>notes</b>	This column contains additional information, including if data were sent by authors, if any column above has data that is not from the main source (i.e. FishBase), how certain metrics were calculated, alternative common names, comments on the experimental protocol, information on conversion to standard " <b>unit</b> ", source of the data (literature search or cited in paper from literature search)	G, T <sub>opt</sub> , C, M
<b>reference</b>	Source (See Table S2).	G, T <sub>opt</sub> , C, M

**Table S2.** Species, common name, the data set(s) in which they appear and the sources (G=growth data, T<sub>opt</sub>=optimum growth temperature data, C=maximum consumption data, M=metabolism data). If more than one data and source, the sources are in order (1 study per species and rate).

Species	Common name	Datasets	Source
<i>Pseudopleuronectes yokohamae</i>	Marbled flounder	G, T <sub>opt</sub> , C	(5)
<i>Cyclopterus lumpus</i>	Lumpfish	G, T <sub>opt</sub>	(6)
<i>Paralichthys olivaceus</i>	Japanese flounder (alt. bastard halibut, Japanese halibut or Olive flounder)	G, T <sub>opt</sub> , C	(7)
<i>Salvelinus alpinus</i>	Arctic char	G, T <sub>opt</sub>	(8)
<i>Salmo salar</i>	Atlantic salmon	G, T <sub>opt</sub>	(9)
<i>Lates calcarifer</i>	Barramundi	G, T <sub>opt</sub> , C, M	(10) (10) (10) (11)
<i>Gadus morhua</i>	Atlantic cod	G, T <sub>opt</sub> , M	(12)(13)
<i>Hippoglossus hippoglossus</i>	Atlantic halibut	G, T <sub>opt</sub>	(14)
<i>Scophthalmus maximus</i>	Turbot	G, T <sub>opt</sub>	(15)
<i>Boreogadus saida</i>	Arctic cod	G, T <sub>opt</sub>	(16)
<i>Rachycentron canadum</i>	Cobia	G, T <sub>opt</sub> , C	(17)
<i>Pelteobagrus fulvidraco</i>	Yellow catfish	G, T <sub>opt</sub> , C	(18)
<i>Anarhichas minor</i>	Spotted wolffish	G, T <sub>opt</sub>	(19)
<i>Oncorhynchus mykiss</i>	Rainbow trout	C, M	(20)
<i>Perca fluviatilis</i>	Eurasian perch	C	(21)
<i>Phoxinus phoxinus</i>	Eurasian minnow	C, M	(22)
<i>Coregonus hoyi</i>	Bloater	C	(23)
<i>Pomoxis annularis</i>	White crappie	C	(24)
<i>Gambusia affinis</i>	Western mosquitofish	C	(25)
<i>Morone saxatilis</i>	Striped bass	C	(26)
<i>Salvelinus fontinalis</i>	Brook trout	C, M	(27) (28)
<i>Leuciscus leuciscus</i>	Dace	C	(29)
<i>Lepomis microlophus</i>	Redear sunfish	C	(30)
<i>Channa argus</i>	Chinese snakehead (alt. Northern snakehead or Snakehead)	C, M	(31) (32)
<i>Siniperca chuatsi</i>	Mandarin fish	C, M	(31) (32)
<i>Gasterosteus aculeatus</i>	Three-spined stickleback	C	(33)
<i>Salmo trutta</i>	Brown trout	C	(34)
<i>Epinephelus coioides</i>	Orange-spotted grouper	C	(35)
<i>Coregonus albula</i>	Vendace	M	(36)
<i>Coregonus fontanae</i>	Stechlin cisco	M	(36)
<i>Abramis brama</i>	Common bream	M	(36)
<i>Rutilus rutilus</i>	Common roach	M	(36)
<i>Salvelinus confluentus</i>	Bull trout	M	(37)
<i>Catostomus commersonii</i>	White sucker	M	(28)
<i>Cyprinus carpio</i>	Common carp	M	(28)
<i>Ameiurus nebulosus</i>	Brown bullhead	M	(28)
<i>Silurus meridionalis</i>	Southern catfish	M	(38)
<i>Carassius auratus</i>	Goldfish	M	(39)
<i>Pomadasys commersonii</i>	Spotted grunter	M	(40)

<i>Melanogrammus aeglefinus</i>	Haddock	M	(41)
<i>Centropristes striata</i>	Black sea bass	M	(42)
<i>Anguilla anguilla</i>	European eel	M	(43)
<i>Micropterus salmoides</i>	Largemouth bass	M	(44)
<i>Cyprinodon macularius</i>	Desert pupfish	M	(45)
<i>Micropogonias undulatus</i>	Atlantic croaker	M	(46)
<i>Leiostomus xanthurus</i>	Spot	M	(46)
<i>Coreius guichenoti</i>	Largemouth bronze gudgeon	M	(47)
<i>Sprattus sprattus</i>	European sprat	M	(48)
<i>Plectropomus leopardus</i>	Leopard coral grouper	M	(49)
<i>Galaxias maculatus</i>	Common galaxias	M	(50)
<i>Polyodon spathula</i>	American paddlefish (alt. Mississippi paddlefish)	M	(51)
<i>Argyrosomus japonicus</i>	Mulloway	M	(52)
<i>Lythrypnus dalli</i>	Bluebanded goby	M	(53)
<i>Collossoma macropomum</i>	Tambaqui (alt. Cachama)	M	(54)
<i>Carassius auratus grandoculis</i>	Round crucian carp (alt. Nigorobuna)	M	(55)

**Table S3.** Description of model parameters (type and their interpretation in brackets) and their prior distributions (see ‘Model description’ and equations 1-3 in the main text).  $N$  refers to a normal distribution (mean and standard deviation, s.d.) and  $U$  to a uniform distribution (interval). For simplicity, only the parameters of the full model are shown here (i.e., with most coefficients varying by species), but note that when a model is fitted with a common rather than species-varying coefficient, for example  $\beta_1$  instead of  $\beta_{1j} \sim N(\mu_{\beta_1}, \sigma_{\beta_1})$ , we use the same prior for  $\beta_1$  as for  $\mu_{\beta_1}$ .

Model	Parameter	Description	Prior distribution
<b>Log-linear regressions for growth, consumption and metabolism</b>	$\mu_{\beta_{0s}}$	Hyperparameter (average intercept for standard metabolic rate across species) <i>Only for metabolism model.</i>	$N(-2, 5)$
	$\mu_{\beta_{0r}}$	Hyperparameter (average intercept for routine and resting metabolic rate across species). <i>Only for metabolism model.</i>	$N(-1, 5)$
	$\mu_{\beta_0}$	Hyperparameter (average intercept across species). <i>Only for consumption and growth models.</i>	$N(0, 5)$
	$\mu_{\beta_1}$	Hyperparameter (average mass coefficient across species)	$N(-0.25, 1)$
	$\mu_{\beta_2}$	Hyperparameter (average temperature coefficient across species)	$N(-0.6, 1)$
	$\mu_{\beta_3}$	Hyperparameter (average interaction coefficient across species)	$N(0, 1)$
	$\sigma_{\beta_{0s}}$	Hyperparameter (s.d. of species-intercepts for standard metabolic rate)	$U(0, 10)$
	$\sigma_{\beta_{0r}}$	Hyperparameter (s.d. of species-intercepts for routine and resting metabolic rate)	$U(0, 10)$
	$\sigma_{\beta_1}$	Hyperparameter (s.d. of species mass coefficients)	$U(0, 10)$
	$\sigma_{\beta_2}$	Hyperparameter (s.d. of species temperature coefficients)	$U(0, 10)$
	$\sigma_{\beta_3}$	Hyperparameter (s.d. of species interaction coefficients)	$U(0, 10)$
	$\sigma$	Parameter (s.d.)	$U(0, 10)$
<b>Sharpe-Schoolfield (unimodal consumption data)</b>	$\mu_{C_{0j}}$	Hyperparameter (average consumption at reference temperature [-10 on centered scale] across species)	$N(1, 1)$
	$\mu_{E_j}$	Hyperparameter (average activation energy across species)	$N(0.5, 0.5)$
	$E_h$	Parameter (common rate of decline with temperature)	$N(2, 2)$
	$T_h$	Parameter (common temperature at which half the rate is reduced due to high temperatures)	$N(5, 2)$
	$\sigma_{E_j}$	Hyperparameter (s.d. of species-varying activation energies)	$U(0, 3)$
	$\sigma_{C_{0j}}$	Hyperparameter (s.d. of species-varying average consumption)	$U(0, 3)$
	$\sigma$	Parameter (s.d.)	$U(0, 3)$
<b>Linear</b>	$\mu_{\beta_0}$	Hyperparameter (average intercept across species)	$N(0, 5)$

<b><math>T_{opt}</math> models</b>	$\mu_{\beta_1}$	Hyperparameter (average mass coefficient across species)	$N(0, 5)$
	$\sigma_{\beta_0}$	Hyperparameter (s.d. of species-intercepts)	$U(0, 10)$
	$\sigma_{\beta_1}$	Hyperparameter (s.d. of species mass coefficients)	$U(0, 10)$
	$\sigma$	Parameter (s.d.)	$U(0, 10)$

**Table S4.** Model comparison for the log-linear regressions of how consumption, metabolism and growth depend on mass and temperature below optimum temperatures (see ‘*Model description*’ and equations 1-3 in the main text). The column m\*t indicates whether the model for the rate includes an interactive effect of mass and temperature. The models differ in which coefficients vary among species and which are common, where  $\beta_0$  is the intercept,  $\beta_1$  mass coefficient (mass-exponent on linear scale),  $\beta_2$  temperature coefficient (corresponding to the negative activation energy) and  $\beta_3$  interaction between mass and temperature. The WAIC columns shows  $\Delta\text{WAIC}$  and absolute WAIC in brackets, rounded to the nearest decimal, where  $\Delta\text{WAIC}$  is the difference between each models’ WAIC and the lowest WAIC across models. Bold indicates models with  $\Delta\text{WAIC} < 2$ .

Model	m*t	Species-varying parameter(s)	WAIC metabolism	WAIC consumption	WAIC growth
<b>M1</b>	Yes	$\beta_0, \beta_1, \beta_2, \beta_3$	<b>0 (273.2)</b>	4.3 (564.5)	<b>0 (47.2)</b>
<b>M2</b>		$\beta_0, \beta_1, \beta_2$	<b>1.27 (274.5)</b>	3.1 (563.4)	7.2 (54.4)
<b>M3a</b>		$\beta_0, \beta_1$	306.1 (579.3)	148.1 (708.4)	23.4 (70.6)
<b>M3b</b>		$\beta_0, \beta_2$	387.5 (660.7)	70.1 (630.4)	32.6 (79.8)
<b>M4</b>		$\beta_0$	649.6 (922.8)	189.9 (750.2)	43.5 (90.7)
<b>M5</b>		$\beta_0, \beta_1, \beta_2$	5.0 (278.2)	<b>0 (560.2)</b>	5.5 (52.7)
<b>M6a</b>	No	$\beta_0, \beta_1$	347.8 (621.0)	166.1 (726.3)	22.1 (69.3)
<b>M6b</b>		$\beta_0, \beta_2$	388.9 (662.1)	74.1 (634.4)	34.3 (81.5)
<b>M7</b>		$\beta_0$	682.2 (955.4)	213.9 (774.2)	44.9 (92.1)

**Table S5.** Comparison of the two models fitted to optimum growth temperature data. The WAIC columns shows  $\Delta$ WAIC and absolute WAIC in brackets, rounded to the nearest decimal, where  $\Delta$ WAIC is the difference between each models' WAIC and the lowest WAIC across models. Bold indicates models with  $\Delta$ WAIC < 2.

Model	Species-varying parameter(s)	WAIC
M1	$\beta_0, \beta_1$	<b>0 (177.3)</b>
M2	$\beta_0$	<b>1 (178.3)</b>

## SI References

1. D. Deslauriers, S. R. Chipps, J. E. Breck, J. A. Rice, C. P. Madenjian, Fish Bioenergetics 4.0: An R-Based Modeling Application. *Fisheries* **42**, 586–596 (2017).
2. J. R. Brett, J. E. Shelbourn, C. T. Shoop, Growth rate and body composition of fingerling sockeye salmon, *Oncorhynchus nerka*, in relation to temperature and ration size. *J. Fish. Res. Bd. Can.* **26**, 2363–2394 (1969).
3. R. Froese, J. T. Thorson, R. B. Reyes, A Bayesian approach for estimating length-weight relationships in fishes. *Journal of Applied Ichthyology* **30**, 78–85 (2014).
4. R. Froese, D. Pauly, Editors. *FishBase* (2019).
5. T. Tomiyama, et al., Ontogenetic changes in the optimal temperature for growth of juvenile marbled flounder *Pseudopleuronectes yokohamae*. *Journal of Sea Research* **141**, 14–20 (2018).
6. A. V. Nytrø, et al., The effect of temperature and fish size on growth of juvenile lumpfish (*Cyclopterus lumpus* L.). *Aquaculture* **434**, 296–302 (2014).
7. N. Iwata, K. Kikuchi, H. Honda, M. Kiyono, H. Kurokura, Effects of temperature on the growth of Japanese flounder. *Fisheries science* **60**, 527–531 (1994).
8. S. I. Siikavuopio, A. Foss, B.-S. Saether, S. Gunnarsson, A. K. Imsland, Comparison of the growth performance of offspring from cultured versus wild populations of arctic charr, *Salvelinus alpinus* (L.), kept at three different temperatures. *Aquac Res* **44**, 995–1001 (2013).
9. S. O. Handeland, A. K. Imsland, S. O. Stefansson, The effect of temperature and fish size on growth, feed intake, food conversion efficiency and stomach evacuation rate of Atlantic salmon post-smolts. *Aquaculture* **283**, 36–42 (2008).
10. M. Bermudes, B. Glencross, K. Austen, W. Hawkins, The effects of temperature and size on the growth, energy budget and waste outputs of barramundi (*Lates calcarifer*). *Aquaculture* **306**, 160–166 (2010).
11. B. D. Glencross, M. Felsing, Influence of fish size and water temperature on the metabolic demand for oxygen by barramundi, *Lates calcarifer* (Bloch), in freshwater. *Aquaculture Res* **37**, 1055–1062 (2006).
12. B. Björnsson, A. Steinsson, T. Árnason, Growth model for Atlantic cod (*Gadus morhua*): Effects of temperature and body weight on growth rate. *Aquaculture* **271**, 216–226 (2007).
13. B. Tirsgaard, J. W. Behrens, J. F. Steffensen, The effect of temperature and body size on metabolic scope of activity in juvenile Atlantic cod *Gadus morhua* L. *Comparative Biochemistry and Physiology Part A: Molecular & Integrative Physiology* **179**, 89–94 (2015).
14. B. Björnsson, S. V. Tryggvadóttir, Effects of size on optimal temperature for growth and growth efficiency of immature Atlantic halibut (*Hippoglossus hippoglossus* L.). *Aquaculture* **142**, 33–42 (1996).
15. T. Árnason, B. Björnsson, A. Steinsson, M. Oddgeirsson, Effects of temperature and body weight on growth rate and feed conversion ratio in turbot (*Scophthalmus maximus*). *Aquaculture* **295**, 218–225 (2009).
16. B. J. Laurel, L. A. Copeman, M. Spencer, P. Iseri, Temperature-dependent growth as a function of size and age in juvenile Arctic cod (*Boreogadus saida*). *ICES Journal of Marine Science* **74**, 1614–1621 (2017).
17. L. Sun, H. Chen, Effects of water temperature and fish size on growth and bioenergetics of cobia (*Rachycentron canadum*). *Aquaculture* **426–427**, 172–180 (2014).
18. L. Zhang, Z.-G. Zhao, Q.-X. Fan, Effects of water temperature and initial weight on growth, digestion and energy budget of yellow catfish *Pelteobagrus fulvidraco* (Richardson, 1846). *J Appl Ichthyol* **33**, 1108–1117 (2017).
19. A. K. Imsland, A. Foss, L. O. Sparboe, S. Sigurdsson, The effect of temperature and fish size on growth and feed efficiency ratio of juvenile spotted wolffish *Anarhichas minor*. *J Fish Biology* **68**, 1107–1122 (2006).
20. J. From, G. Rasmussen, A growth model, gastric evacuation, and body composition in rainbow trout, *Salmo gairdneri* Richardson, 1836. *Dana* **3**, 61–139 (1984).
21. O. Lessmark, “Competition between perch (*Perca fluviatilis*) and roach (*Rutilus rutilus*) in south Swedish lakes,” Limnologiska Institutionen, Lunds Universitet (Sweden). (1983).

22. Y. Cui, R. J. Wootton, Bioenergetics of growth of a cyprinid, *Phoxinus phoxinus*: the effect of ration, temperature and body size on food consumption, faecal production and nitrogenous excretion. *J Fish Biology* **33**, 431–443 (1988).
23. F. P. Binkowski, L. G. Rudstam, Maximum Daily Ration of Great Lakes Bloater. *Transactions of the American Fisheries Society* **123**, 335–343 (1994).
24. R. S. Hayward, E. Arnold, Temperature Dependence of Maximum Daily Consumption in White Crappie: Implications for Fisheries Management. *Transactions of the American Fisheries Society* **125**, 132–138 (1996).
25. S. R. Chipp, D. H. Wahl, Development and Evaluation of a Western Mosquitofish Bioenergetics Model. *Transactions of the American Fisheries Society* **133**, 1150–1162 (2004).
26. J. Duston, T. Astatkie, P. F. MacIsaac, Effect of body size on growth and food conversion of juvenile striped bass reared at 16–28 °C in freshwater and seawater. *Aquaculture* **234**, 589–600 (2004).
27. N. S. Baldwin, Food Consumption and Growth of Brook Trout at Different Temperatures. *Transactions of the American Fisheries Society* **86**, 323–328 (1957).
28. F. W. H. Beamish, Respiration of fishes with special emphasis on standard oxygen consumption II. Influence of weight and temperature on respiration of several species'. *Canadian Journal of Zoology/Revue Canadienne de Zoologie* **42**, 177–188 (1964).
29. G. Marmulla, R. Rosch, Maximum daily ration of juvenile fish fed on living natural zooplankton. *J Fish Biology* **36**, 789–801 (1990).
30. H. P. Wang, R. S. Hayward, G. W. Whittlesey, S. A. Fischer, Prey-size Preference, Maximum Handling Size, and Consumption Rates for Redear Sunfish *Lepomis microlophus* Feeding on Two Gastropods Common to Aquaculture Ponds. *J World Aquaculture Soc* **34**, 379–386 (2003).
31. J. Liu, Y. Cui, J. Liu, Food consumption and growth of two piscivorous fishes, the mandarin fish and the Chinese snakehead. *Journal of Fish Biology* **53**, 1071–1083 (1998).
32. J. Liu, Y. Cui, J. Liu, Resting metabolism and heat increment of feeding in mandarin fish (*Siniperca chuatsi*) and Chinese snakehead (*Channa argus*). *Comparative Biochemistry and Physiology Part A: Molecular & Integrative Physiology* **127**, 131–138 (2000).
33. R. J. Wootton, J. R. M. Allen, S. J. Cole, Effect of body weight and temperature on the maximum daily food consumption of *Gasterosteus aculeatus* L. and *Phoxinus phoxinus* (L.): selecting an appropriate model. *J Fish Biology* **17**, 695–705 (1980).
34. J. M. Elliott, The Energetics of Feeding, Metabolism and Growth of Brown Trout (*Salmo trutta* L.) in Relation to Body Weight, Water Temperature and Ration Size. *The Journal of Animal Ecology* **45**, 923 (1976).
35. X. Lin, S. Xie, Y. Su, Y. Cui, Optimum temperature for the growth performance of juvenile orange-spotted grouper (*Epinephelus coioides* H.). *Chin. J. Ocean. Limnol.* **26**, 69–75 (2008).
36. J. Ohlberger, Thomas. Mehner, Georg. Staaks, Franz. Höller, Intraspecific temperature dependence of the scaling of metabolic rate with body mass in fishes and its ecological implications. *Oikos* **121**, 245–251 (2012).
37. M. G. Mesa, L. K. Weiland, H. E. Christiansen, S. T. Sauter, D. A. Beauchamp, Development and evaluation of a bioenergetics model for bull trout. *Transactions of the American Fisheries Society* **142**, 41–49 (2013).
38. Xiaojun. Xie, Ruyung. Sun, The Bioenergetics of the Southern Catfish (*Silurus meridionalis* Chen). I. Resting Metabolic Rate as a Function of Body Weight and Temperature. *Physiological Zoology* **63**, 1181–1195 (1990).
39. F. W. H. Beamish, P. S. Mookherjee, Respiration of fishes with special emphasis on standard oxygen consumption: I. influence of weight and temperature on respiration of goldfish, *Carassius auratus* L. *Can. J. Zool.* **42**, 161–175 (1964).
40. H. Du Perez H., A. McLachlan, J. F. K. Marais, Oxygen consumption of a shallow water teleost, the spotted grunter, *Pomadys commersonni* (Lacépède, 1802). *Comparative Biochemistry and Physiology* **84a**, 61–70 (1986).

41. M. A. Peck, L. J. Buckley, D. A. Bengtson, Effects of temperature, body size and feeding on rates of metabolism in young-of-the-year haddock. *Journal of Fish Biology* **66**, 911–923 (2005).
42. E. Slesinger, *et al.*, The effect of ocean warming on black sea bass (*Centropristes striata*) aerobic scope and hypoxia tolerance. *PLoS ONE* **14**, e0218390 (2019).
43. G. Degani, M. L. Gallagher, A. Meltzer, The influence of body size and temperature on oxygen consumption of the European eel, *Anguilla anguilla*. *J Fish Biology* **34**, 19–24 (1989).
44. D. C. Glover, D. R. DeVries, R. A. Wright, Effects of temperature, salinity and body size on routine metabolism of coastal largemouth bass *Micropterus salmoides*. *Journal of Fish Biology* **81**, 1463–1478 (2012).
45. M. Heuton, *et al.*, Oxygen consumption of desert pupfish at ecologically relevant temperatures suggests a significant role for anaerobic metabolism. *J Comp Physiol B* **188**, 821–830 (2018).
46. A. Z. Horodysky, R. W. Brill, P. G. Bushnell, J. A. Musick, R. J. Latour, Comparative metabolic rates of common western North Atlantic Ocean sciaenid fishes. *Journal of Fish Biology* **79**, 235–255 (2011).
47. Y. P. Luo, Q. Q. Wang, Effects of body mass and temperature on routine metabolic rate of juvenile largemouth bronze gudgeon *Coreius guichenoti*. *Journal of Fish Biology* **80**, 842–851 (2012).
48. L. Meskendahl, J.-P. Herrmann, A. Temming, Effects of temperature and body mass on metabolic rates of sprat, *Sprattus sprattus* L. *Mar Biol* **157**, 1917–1927 (2010).
49. V. Messmer, *et al.*, Global warming may disproportionately affect larger adults in a predatory coral reef fish. *Global Change Biology* **23**, 2230–2240 (2017).
50. D. Milano, P. Vigliano, D. Beauchamp, Effect of body size and temperature on respiration of *Galaxias maculatus* (Pisces: Galaxiidae). *New Zealand Journal of Marine and Freshwater Research* **51**, 295–303 (2016).
51. J. T. Patterson, S. D. Mims, R. A. Wright, Effects of body mass and water temperature on routine metabolism of American paddlefish *Polyodon spathula*: routine metabolism of *Polyodon spathula*. *J Fish Biol* **82**, 1269–1280 (2013).
52. I. Pirozzi, M. A. Booth, The effect of temperature and body weight on the routine metabolic rate and postprandial metabolic response in muloway, *Argyrosomus japonicus*. *Comparative Biochemistry and Physiology Part A: Molecular & Integrative Physiology* **154**, 110–118 (2009).
53. R. E. Rangel, D. W. Johnson, Metabolic responses to temperature in a sedentary reef fish, the bluebanded goby (*Lythrypnus dalli*, Gilbert). *Journal of Experimental Marine Biology and Ecology* **501**, 83–89 (2018).
54. D. Tomala, J. Chavarria, B. Angeles, Evaluacion de la tasa de consumo de oxigeno de *Colossoma macropomum* en relacion al peso corporal y temperatura del agua. *Iajar* **42**, 971–979 (2014).
55. H. Yamanaka, T. Takahara, Y. Kohmatsu, M. Yuma, Body size and temperature dependence of routine metabolic rate and critical oxygen concentration in larvae and juveniles of the round crucian carp *Carassius auratus grandoculis* Temminck & Schlegel 1846. *J. Appl. Ichthyol.* **29**, 891–895 (2013).